Regulation of Apelin Is Associated with Proliferation and Angiogenesis in Gastric Cancer

LiJun Tian
Binzhou Medical College: Binzhou Medical University
Hong-Zhi Liu
Binzhou Medical College: Binzhou Medical University
Qiang Zhang
Binzhou Medical College: Binzhou Medical University
Dian-Zhong Geng
Binzhou Medical College: Binzhou Medical University
Jing Yang
Binzhou Medical College: Binzhou Medical University
Hai-Tao Geng
Binzhou Medical College: Binzhou Medical University
Yu-Jie Zhai
Binzhou Medical College: Binzhou Medical University
Yu-Qing Huo
Binzhou Medical College: Binzhou Medical University
YanZhang Hao (byfyzly@163.com)
Binzhou Medical College affiliated Hospital

Research

Keywords: Apelin, gastric cancer, tumor growth, signal pathway

Posted Date: November 13th, 2020

DOI: https://doi.org/10.21203/rs.3.rs-104563/v1

Abstract

Background: Apelin is an emerging endogenous ligand, which is involved in proliferation and angiogenesis in certain cancers. However, few studies have reported its functions and underlying mechanisms in human gastric cancer (GC). Therefore, the present study aimed to investigate the effect of Apelin expression in human GC and the underlying mechanisms of Apelin in the promotion of proliferation both *in vitro* and *in vivo*.

Methods: A total of 178 patients diagnosed with GC under postoperative care were enrolled for the study to investigate clinicopathological and immunohistochemical factors of Apelin expression. Survival of patients was analyzed using the Kaplan-Meier method and Cox regression model. We adopted quantitative real-time reverse transcription-polymerase chain reaction (RT-PCR), western blot and ELISA to analyze human GC specimens and cell lines. The role and mechanisms of Apelin were evaluated by performing *in vitro* and *in vivo* experiments to analyze exogenous Apelin and its overexpression in human GC cells.

Results: The expression of Apelin was higher in human gastric cancer cells than in adjacent normal tissues. Apelin, which was overexpressed in vessel invasion (P <0.01), lymph node metastasis (P <0.01), late-staged tumor (T) status (P <0.05), pathological type (P <0.05) and nerve invasion (P <0.05), also exhibited a positive correlation with vascular endothelial growth factor (VEGF). Apelin overexpression or exogenous Apelin activated downstream of ERK/Cyclin D1/MMP-9 signaling pathway to promote MGC-803 cell proliferation and invasion *in vitro*. Apelin overexpression promoted angiogenesis aiming at accelerating growth of subcutaneous xenograft *in vivo*.

Conclusions: This study has elucidated the relationship between Apelin and its clinicopathological features in human GC, and the role of Apelin in tumor cell proliferation in human GC cell lines. This is the first study to elucidate underlying mechanisms of Apelin in the proliferation of GC. Apelin can be a potential therapeutic target for human GC.

Background

Gastric cancer (GC) is the fifth most common and aggressive malignancy, which causes a third of cancer-related mortality globally [1, 2]. In spite of the advancement in therapeutic approaches including radical surgical resection, adjuvant chemoradiation and targeted therapy, the prognosis for GC patients remains poor and an overall 5-year survival rate is approximately 20–40% [3–5]. There is no characteristic and definite molecular marker that can facilitate diagnosis and prognosis prediction for early-staged GC, although a few previous findings have suggested that a series of proteins could be associated with the clinical outcomes of patients diagnosed with GC [6, 7].

The bioactive peptide Apelin is an emerging endogenous ligand, which binds to the human G protein-coupled receptor APJ [8]. Apelin is a member of the adipokine family that is secreted by adipose tissue, and its expression is also observed in various cell types [9]. The Apelin gene encodes a prepropeptide

consisting of 77 amino acids that may promote proteolytic maturation and subsequently generate different bioactive peptide fragments: Apelin-17, Apelin-36 and Apelin-13 that are the predominant types in the human plasma [8, 9]. Apelin/APJ signaling pathway, which is widely expressed in the cardiovascular system, has been reported to be involved in various physiological and pathological processes such as angiogenesis, heart failure, energy metabolism and cancer progression[9, 10]. The dysfunctional, abnormal vasculature morphology plays a significant role in the growth and development of tumor [10–12]. Previous studies have revealed that VEGF and its receptor are instrumental in angiogenesis, and have been used as a therapeutic target for over 30 years [11, 12]. Apelin overexpression stimulates proliferation of endothelial cells, enhances tumor vascularization and formulates capillary tubes both *in vivo* and *in vitro*[13, 14]. In addition, Apelin upregulation has been reported in previous studies, and strikingly, a correlation between the level of Apelin expression and clinical outcomes in specific human cancers has been observed[15, 16].

However, there are few studies on the role and molecular mechanisms of Apelin in GC. Therefore, the present study aimed to investigate the correlation between Apelin expression and clinical outcomes in human GC by performing a retrospective study, and to reveal the role and underlying molecular mechanisms of Apelin in GC cells *in vitro* and in mice.

Patients And Methods

Patients

A retrospective study was conducted using surgical specimens by comparing tumor tissues and adjacent normal tissues obtained from 178 patients with histopathologically confirmed GC from Binzhou Medical College Affiliated Hospital. The clinicopathological data of patients covered the period between January 2009 and December 2011. The patients underwent radical surgical resection with D2 lymphadenectomy and were subjected to chemotherapy with or without radiotherapy. All patients were required to undergo computed tomography (CT) scanning for the neck, chest and abdomen, and anti-tumor therapies could not be administered before surgery. Postoperative chemotherapy began 1 month after surgery and included treatment with fluoropyrimidine or capecitabine in combination with oxaliplatin or paclitaxel, repeated for at least 4 cycles. Eligible patients underwent radiotherapy by adopting intensive modulation radiotherapy (IMRT) and the prescribed dose was 45-50.4 Gy given as 1.8-2.0 Gy per fraction. The progression-free survival (PFS) time corresponded with the period from the beginning of operation to the occurrence of disease progression, death or the end of the study. Overall survival (OS) corresponded to the period from surgery to death or December 31, 2016.

Immunohistochemical analysis

Immunohistochemical analyses were performed on tumor tissues previously fixed in formalin and embedded in paraffin. The tissue sections (4 μm) were deparaffinized with xylene and rehydrated in gradients of alcohol. Heat-induced antigen retrieval was performed in 0.0 l M citrate buffer (PH = 6) for 5 minutes and subsequently the slides were heated in a microwave oven for 15 minutes. Tissue sections

were incubated in 3% H_2O_2-methanol solution to block endogenous peroxidase at 37.0 °C for 20 minutes. After blocking with albumen for 10 minutes, the sections were incubated overnight at 4 °C with anti-Apelin, anti-VEGF or anti-CD34 antibodies at dilution ratios of 1:200, 1:100 or 1:200, respectively (Abcam, the USA). The EnVision-HRP detection system (Dako, Carpinteria, CA, the USA) was used to evaluate the tissues, with diaminobenzidine as the chromogen and Mayer's modified hematoxylin as the counterstain. Tissues were incubated with 80 μL goat anti-rabbit or rabbit anti-mouse immunoglobulin G (IgG) (Dako, Carpinteria, CA, the USA) labeled with horseradish peroxidase using a dilution ratio of 1:250 at 37 °C for 30 minutes. The tissues were evaluated by two investigators who were blinded to clinical data. The investigators initially disagreed on the evaluation of approximately 10% of the tissues but they reached a consensus after further consultations. Apelin or VEGF immunostaining score was calculated by multiplying the positive cell area score and the staining intensity score. An immunoexpression score > 3 was considered positive, whereas a score ≤ 3 was considered negative. The staining intensity score was classified into four levels: no staining (0), light yellow staining (1), yellow staining (2) and deep yellow staining (3). The positive cell area score was based on the percentage of positive cells and was classified as follows: no positivity (0), less than 10% positivity (1), 11–50% positivity (2), 51–75% positivity (3) and more than 76% positive cells (4) [15, 16]. Microvessel densities (MVD) were established by labeling capillaries (0.02–0.10 mm) with CD34 (Dako, Carpinteria, CA, the USA). Morphometric analysis was performed on three sections per slide using computer-aided CUE-2 software (Olympus Vanox, Tokyo, Japan) as previously described [17].

Cell culture

Human GC cell lines HGC-27, MGC-803, and SGC-7901 were obtained from Anhui Medical University (Anhui, China). All cell lines were cultured in DMEM (Gibco, CA, the USA) supplemented with 10% FBS (Gibco, CA, the USA) at 37ºC and 5% CO_2.

Construction of stable transfected cell lines

Apelin complementary DNA was purchased from Thermo Fisher Scientific (Shanghai, China). DNA encoding areas were amplified using the following primers: 5'-CGCGAATTCGGCATGAATCTGCGGCTCTG-3'and 5'-GCGCTCGAGTCAGAAAGGCATGGGTCC-3'. The amplified PCR products were subcloned with Apelin cDNA into the pcDNA 3.1 vector adopting *Eco*RI and *Xho*I restriction enzymes (Invitrogen, Carlsbad, CA, USA). Vector expression was verified through DNA sequencing. An empty vector or an Apelin-encoding pcDNA 3.1 vector was transfected into the MGC-803 cell line, which has been demonstrated to express a relatively low level of Apelin using Lipofectamine 2000 transfection reagent (Thermo Fisher Scientific, Shanghai, China) according to the manufacturer's protocol.

RNA isolation and quantitative real-time reverse transcription-polymerase chain reaction

Total RNA was isolated from each human GC cell line with TRIzol reagent (Invitrogen, Carlsbad, CA, the USA) in accordance with the manufacturer's guidelines. It was reverse-transcribed into cDNA using the murine leukemia virus reverse transcriptase. PCR amplifications were carried out under the following

cyclic conditions: 42 cycles of incubation at 95 °C for 20 seconds and at 60 °C for 30 seconds. PCR products were visualized by electrophoresis on 2% agarose gels stained with ethidium bromide. The primers for PCR were: Apelin, 5'-GATGCCGCTTCCCGATG-3'(forward) and 5'-ATTCCTTGACCCTCTGGGCT-3'(reverse); β-actin, 5'-TGCTGTCCCTGTATGCCTCT-3' (forward) and 5'-AGGTCTTTACGGATGTCAACG-3' (reverse). The mRNA levels were calculated with the $2^{-\Delta\Delta Ct}$ method [18]. Gene expression level of Apelin mRNA in MGC-803 cell line was determined using the same method at 48 hours after transfection with control or Apelin-encoding pc DNA 3.1 vector.

Protein Extraction and Western Blot analysis

Cultured cells at logarithmic growth phase were resuspended in lysis buffer containing 5μL Protease Inhibitor Cocktail (cOmplete, Sigma, Germany) and then lysed as described previously [19]. The protein concentration in the supernatants was measured using the Bradford protein assay kit (Bio-Rad, Hercules, CA, the USA). Equivalent amounts of protein samples (80 μg/lane) were fractionated on 10% sodium dodecyl sulfate (SDS)-polyacrylamide gel and transferred onto polyvinylidene fluoride (PVDF) membranes at 0.8 mA/cm^2 for 20–30 minutes. The membranes were blocked with Tris-buffered saline (TBS) containing 10% nonfat milk at 37 °C for 2 hours, and incubated with primary antibodies against Apelin, β-actin, pERK, pAkt, Cyclin D1 and MMP-9 at 4 °C overnight. Membranes were washed four times with TBST, and then incubated with horseradish peroxidase (HRP)-conjugated secondary antibodies for 2 hours at 37.0 °C. The blots were visualized using the ECL reagent and quantified using Quantity One software. The primary antibodies were used at the following dilutions: 1:200 (Apelin, Phoenix Pharmaceuticals, the USA), 1:2,000 (β-actin, Maxim, China), 1:200 (pERK, Cell Signaling Technology, France), 1:1000 (pAkt, Santa Cruz Biotechnology, the USA), 1:200 (Cyclin D1, Santa Cruz Biotechnology) and 1:200 (MMP-9, Santa Cruz Biotechnology). Proteins were isolated from MGC-803 cells for western blotting after 48 hours of transfection with pcDNA3.1-Apelin or control vector and induction by Apelin-13 (Phoenix Pharmaceuticals, Inc, the USA). The expression of pERK, pAkt, Cyclin D1 and MMP-9 in MGC-803 cells was performed in aforementioned method.

ELISA

Equal amount (500μL) of MGC-803 cell culture supernatants were collected in duplicate and the concentration of Apelin was measured using human Apelin ELISA kit (Phoenix Pharmaceuticals, the USA) following the manufacturer's instructions. Similarly, we determined the concentration change of Apelin after transfection with pcDNA3.1-Apelin or control vector in this way.

Cell Proliferation Studies

To assess cell proliferation, 1×10^4 cells per well were seeded in triplicate onto flat-bottomed 96-well microplates and cultured for 24 hours. The cells were synchronized for 12 hours in DMEM containing 0.5% FBS. After addition of different concentrations of Apelin-13 (0.02 μmol/L, 0.1 μmol/L, 0.5 μmol/L, 2.5 μmol/L 12.5 μmol/L, 62.5 μmol/L) for 24 hours, the cells were treated with MTT (5 mg/mL) at 37.0 °C for 4 hours. The 150μL dimethyl sulfoxide (DMSO) was added to each well to remove cells that were not

reduced by MTT reagent. The absorbance of cell supernatants was measured at 570 nm using a microplate reader (Thermo Multiskan Ascent, the USA). We would also measure the absorbance at 570 nm using the optimal concentration obtained from the previous experiment at different time points (6 h, 12 h, 24 h, 36 h, 48 h). For certification the change of cell proliferation after transfection with pcDNA 3.1 or pcDNA 3.1-Apelin vector into MGC-803 cells, we also measured the absorbance at 570 nm at different time points as mentioned.

Cell Migration and Invasion Analysis

Transwell chambers (BD, the USA) were used to study cell migration and invasion. MGC-803 cells were divided into 4 groups and prepared in triplicate: cells without treatment, cells treated with Apelin-13, cells transfected with pcDNA 3.1, and cells transfected with pcDNA 3.1-Apelin. The 5×10^4 cells were seeded in the upper chamber, which was in advanced scribbled with Matrigel (BD, the USA), containing a medium without serum. The 600μL 10% DMEM were added in the lower chamber. The Transwell chambers were incubated for 24 hours. Next, cells that did not invade the membrane were removed. Those that invaded were stained with 4% polyoxymethylene for 15 minutes and then with 0.2% crystal violet, and counted under an inverted microscope at 200 × magnification (Olympus, Japan).

Detection Apoptosis in MGC-803 cell with Flow Cytometry

Suberoylanilide hydroxamic acid (SAHA), which induces apoptosis of MGC-803 cells [20], is a member of histone deacetylase inhibitor (HDACI) family. Its optimal concentration of inducing apoptosis of MGC-803 cells was 2 μmol/L treated for 24 hours [20]. MGC-803 cells were divided into 5 subgroups: untreated cells, cells treated with SAHA (2 μmol/L for 24 hours), cells treated with SAHA + Apelin-13 (2.5 μmol/L for 24hours), cells treated with SAHA + pcDNA3.1 (24hours after transfection), and cells treated with SAHA + pcDNA3.1-Apelin (24hours after transfection). Cells were treated with different agents and resuspended in 300μL of binding buffer of the Annexin V-FITC apoptosis detection kit (BD, the USA). Subsequently, cells were mixed with 5μL of Annexin V-FITC for 15 minutes and then 5μL of propidium iodide (PI) at 37.0 °C for 5 minutes both in the dark. Finally, cells were mixed with 200μL of binding buffer and examined by flow cytometry (BD, the USA). U1 subset (meaning Annexin V-FITC (-)/PI (+)) stood for necrosis, meanwhile U2 subset (meaning Annexin V-FITC (+)/PI (+)) represented late-staged apoptosis. U3 subset (meaning Annexin V-FITC (-)/PI (-)) stood for control, but U4 subset (meaning Annexin V-FITC (+)/PI (-)) represented early-staged apoptosis. The rate of apoptosis was calculated as: (U2 + U4) / (U1 + U2 + U3 + U4) × 100%.

Construction of Apelin-stable-transfection of MGC-803 cell

To determine the optimal concentration of puromycin (Beijing Inovogen Tech.Co. Ltd, China), cells growing at a logarithmic phase were cultured in 24-well microplates at a density if 2×10^4 cells/well overnight and then mixed with different concentrations of puromycin (0, 1, 2.5, 5, 7.5, 10, 15 μg/mL). Puromycin at 7.5 μg/mL (the lowest concentration) killed all MGC-803 cells after 72 hours of treatment. This concentration, regarded as optimal concentration, was chosen for subsequent experiments. MGC-803 cells were seeded and cultured in 24-well plates with DMEM without FBS or antibiotic until the plate

became 80% confluent. The 2 mL polybrene (Beijing Inovogen Tech.Co.Ltd. China) (final concentration 6 μg/mL) and viral supernatant 0.5 mL were added to each well and cultured at 37 °C for 4 hours. Fresh DMEM was added into each well for incubation at 37 °C for 24 hours. Three days after transfection, a medium containing puromycin (7.5 μg/mL) was added to each well and cultured at 37 °C. The medium was changed every 2–3 days until colonies were formed. Negative colonies were removed, and the remaining puromycin-resistant colonies were transferred to a 24-well microplate to cover an area nearly more than half of the dish. mRNA and protein expression of target genes were determined with RT-PCR and Western blot assays.

Subcutaneous xenografts in vivo

Fourteen nude mice (BALB/c nu/nu, female, 5–6 weeks old, obtained from the Laboratory Animal Resources of Chinese Academy of Sciences, Shanghai, China) were raised in pathogen-free conditions. The xenograft tumors were established by subcutaneous injection of 0.2 mL MGC-803 cells (1×10^7/mL) stably expressing Apelin or control into the mice. The long diameter (a), short diameter (b), and weight of tumor were measured twice a week by the same investigator. The tumor volumes (mm^3) was calculated using the following formula: $V = ab^2/2$. Values obtained were used to plot a tumor growth curve. Mice were euthanized after 35 days of xenograft tumors formation for further examination. The tumor proliferation rate was calculated as: (the averaged weight of xenograft tumors in the experiment -the averaged weight of control group)/ the averaged weight of xenograft tumors × 100%.

Immunohistochemistry of MVD in Vivo

Immunohistochemical staining was performed for MVD in murine tumors as described previously in this study.

Statistical Analysis

All statistical analyses were performed using SPSS version 16.0 (IBM Corp., Armonk, NY, the USA). The chi-square test was employed to analyze the correlation of clinicopathologic factors with Apelin and VEGF expression. Continuous variables such as MVD were expressed as mean ± S.E.M. Differences between the two groups were determined by Student *t*-test or nonparametric tests. The association between Apelin-encoding protein and VEGF-encoding protein expression was analyzed by Spearman's rank correlation test. Kaplan-Meier analysis and Cox proportional hazards were used to draw survival curves, and log-rank test to assess survival rates. $P < 0.05$ was regarded statistically significant.

Results

The results revealed that there were 141 males and 37 females, with a median age of 62 years (range 34–38 years). The number of patients with the primary lesion site localized to the cardiac region, gastric fundus, gastric body and gastric antrum was 61, 14, 49 and 54, respectively. The histological types of tumor cells were divided into 4 categories based on the degree of tumor differentiation: well or moderately differentiated (82 cases), poorly differentiated (75 cases), mucinous adenocarcinoma (17

cases) and signet ring cell carcinoma (2 cases). Tumor stages for all patients were redefined according to pathological outcomes, which were based on the AJCC/UICC TNM classification revised in 2010. Five patients were staged I, 98 patients were stage II and 75 patients were staged III cancer.

Immunohistochemical analyses were performed to detect protein expression levels of Apelin in 53 of 178 normal gastric tissues adjacent to tumor tissues, while 88 of 178 tumor tissues were analyzed by immunohistochemical staining (29.78% vs 49.44%, $P < 0.001$, Table 1.1). Additionally, the immunoreactivity of Apelin exhibited a diffuse cytoplasmic immunostaining in tumor tissues (Fig. 1.1). Similarly, the percentage of VEGF-positive tumor cells was significantly higher in tumor tissues than in adjacent normal tissues, which was consistent with previous studies (55.62% vs 39.89%, $P = 0.003$, Table 1.1). Furthermore, immunoexpression of VEGF protein exhibited a cytoplasmic pattern consistent with Apelin (Fig. 1.2).

Table 1.1
Expression of Apelin and VEGF in gastric cancer tissues and adjacent tissues

		cancer tissues	adjacent tissues	χ^2 value	*P* value
Apelin	positive	88	53	14.386	0.001
	negative	90	125		
VEGF	positive	99	71	8.827	0.003
	negative	79	107		

A chi-square test was used to investigate the correlations between clinicopathological factors and Apelin and VEGF expression. Apelin expression was significantly positively correlated with vessel invasion and lymph node metastasis ($P < 0.01$), ($P < 0.01$) (Table 1.2). In addition, significant positive correlations were observed between Apelin expression and late-staged tumor (T) status, pathological type, and nerve invasion ($P < 0.05$). Conversely, no significant associations were observed between Apelin expression and gender, age, and the site of primary lesion ($P > 0.05$). VEGF expression was significantly high during late T stage ($P < 0.01$), vessel invasion and positive N stage ($P < 0.05$); however, no statistically significant difference was observed between VEGF expression and gender, age, the site of primary lesion, pathological type and nerve invasion ($P > 0.05$).

Table 1.2
The relationship between Apelin and VEGF and clinicopathologic factors

Characteristics	Apelin		χ^2	*P value*	VEGF		χ^2	*P value*
	+ (n)	- (n)	value		+ (n)	- (n)	value	
Gender			1.001	0.317			0.810	0.368
Male	67	74			76	65		
Female	21	16			23	14		
Age(years)			0.840	0.772			1.585	0.208
≤ 62	46	49			57	38		
62	42	41			42	41		
site of primary lesion			3.240	0.356			6.420	0.093
Cardia	28	33			26	35		
Fundus	7	7			9	5		
Body	21	28			31	18		
Antrum	32	22			33	21		
Pathological differentiation			11.240	0.024			5.103	0.277
Well or moderately differentiated	33	49			43	39		
Poorly differentiated	42	33			42	33		
Mucinous adenocarcinoma	11	6			10	7		
Signet ring cell carcinoma	0	2			2	0		
Other	2	0			2	0		
Nerve invasion			5.731	0.017			3.116	0.078
Yes	49	34			52	31		
No	39	56			47	48		
Vessel invasion			7.910	0.005			5.807	0.016
Yes	38	21			40	19		
No	50	69			59	60		
T stage			9.845	0.020			11.597	0.009
T1	1	1			1	1		

Characteristics	Apelin		χ^2 value	*P value*	VEGF		χ^2 value	*P value*
	+ (n)	- (n)			+ (n)	- (n)		
T2	2	11			3	10		
T3	58	63			64	57		
T4	27	15			31	11		
N stage			14.433	0.002			8.653	0.034
N0	18	23			21	20		
N1	13	26			16	23		
N2	22	27			35	14		
N3	35	14			27	22		

A statistically significant difference was observed in the Apelin-positive subgroup with high MVD expression (33.086 ± 7.862; $P < 0.05$) compared to the Apelin-negative tumor tissues with low MVD expression (21.071 ± 6.320). Similarly, a statistically significant difference was observed between the VEGF-positive subgroup with high MVD expression (29.075 ± 8.193) and VEGF-negative subgroup with low MVD expression (19.638 ± 5.614; $P < 0.05$) (Table 1.3 and Fig. 1.3).

Table 1.3
The relationship between the expression of Apelin, VEGF and MVD

Characteristics		MVD	*t*	*P*
Apelin	positive	33.086 ± 7.862	2.917	0.013
	negative	21.071 ± 6.320		
VEGF	positive	29.075 ± 8.193	2.514	0.025
	negative	19.638 ± 5.614		

The results of immunohistochemical analyses further revealed that the percentage of VEGF-positive expression, 72.7% (64/88) was significantly higher in Apelin-positive tumor cells than in Apelin-negative tumor cells, 38.9% (35/90). Furthermore, Apelin expression was positive in 64 (64.6%) of 99 VEGF-positive patients and 24 (30.3%) of 79 VEGF-negative patients. The results implied a significant positive correlation between Apelin protein expression and VEGF protein expression with relative risks of 0.856 ($P < 0.01$, Table 1.4).

Table 1.4
The association between Apelin and VEGF expression

Characteristics		Apelin		r_s	*P*
		positive	negative	0.856	0.004
VEGF	positive	64	35		
	negative	24	55		

The OS rates of patients with positive expression of Apelin at 1 year, 3 years and 5 years were 97.73%, 62.50% and 28.41%, respectively (Fig. 1.4), whereas the OS rates of patients with negative expression of Apelin at 1 year, 3 years and 5 years were 97.78%, 76.67% and 53.33%, respectively. The median OS time for patients with positive expression of Apelin was 40.7 months and 60.2 months for patients with negative expression of Apelin and a statistically significant difference was observed between the two subgroups ($\chi^2 = 12.549$, $P < 0.001$). The PFS rates between patients with negative expression of Apelin and patients with positive expression of Apelin at 1 year was 94.44% vs 96.60%, at 3 years was 65.56% vs 44.32%, and at 5 years was 40.00% vs 19.32% (Fig. 1.5). A statistically significant difference in the median PFS (49.8 months vs 30.5 months, $\chi^2 = 9.537$, $P = 0.002$) was observed between the two subgroups. Overall, patients in the Apelin-negative subgroups had significantly longer OS and PFS intervals than patients in the Apelin-positive subgroups.

Subsequently, univariate Cox proportional hazards model was used to analyze the effects of various variables on OS. The analysis revealed that Apelin expression, VEGF expression, T stage, lymph node (N) stage, vessel invasion and histological type (all $P < 0.05$) excluding gender, age, the site of primary tumor or nerve invasion (all $P > 0.05$) were significantly associated with poor prognosis (Table 1.5). Multivariate analysis revealed that lymph node metastasis ($P < 0.001$), late-staged status ($P = 0.008$), poor differentiation ($P = 0.027$) and other histological types (including mucinous adenocarcinoma, signet ring cell carcinoma and small cell carcinoma) were independent prognostic factors of poor OS ($P = 0.012$) (Table 1.6).

Table 1.5
COX univariate analysis of factors associated with survival in 178 patients with gastric cancer

Characteristics	5 years overall survival(OS)		
	HR	95%CI	*P* value
Age(years)			0.451
≤ 62	1.000	Ref.	
> 62	1.284	0.786–1.852	
Gender			0.423
Male	1.000	Ref.	
Female	0.936	0.605–1.633	
Position			
Cardia	1.000	Ref.	—
Fundus	0.972	0.112–6.668	0.503
Corpora	0.774	0.276–1.942	0.137
Sinuses	0.865	0.413–1.826	0.257
Pathological differentiation			
Well/moderately differentiated	1.000	Ref.	—
Poorly differentiated	2.336	1.324–3.735	0.030
Other [a]	4.413	1.041–12.546	0.001
Nerve invasion			0.068
No	1.000	Ref.	
Yes	1.258	0.646–2.425	
Vessel invasion			0.025
No	1.000	Ref.	
Yes	2.369	0.983–4.337	
T stages			0.016
T1 + T2	1.000	Ref.	
T3 + T4	3.007	1.353–5.724	

a: Mucinous adenocarcinoma, signet ring cell carcinoma and small cell carcinoma. b: N_1、N_2、N_3

Characteristics	5 years overall survival(OS)		
	HR	95%CI	*P* value
N stages			0.001
N0	1.000	Ref.	
N + [b]	4.591	2.081–8.852	
Apelin			0.001
Negative	1.000	Ref.	
Positive	3.984	1.276–6.824	
VEGF			0.027
Negative	1.000	Ref.	
Positive	2.322	1.020–5.316	
a: Mucinous adenocarcinoma, signet ring cell carcinoma and small cell carcinoma. b: N_1、N_2、N_3			

Table 1.6
Multivariable analysis of the factors associated with survival in 178 patients with gastric cancer

Characteristics	5 years overall survival(OS)		
	HR	95%CI	*P* value
Apelin			0.095
Negative	1.000	Ref.	
Positive	1.226	0.559–2.673	
VEGF			0.139
Negative	1.000	Ref.	
Positive	1.178	0.420–2.569	
Pathological differentiation			
Well/ moderately differentiated	1.000	Ref.	—
Poorly differentiated	2.605	1.228–4.947	0.027
Other[a]	3.239	1.153–10.345	0.012
Vessel invasion			0.069
No	1.000	Ref.	
Yes	1.427	0.698–3.566	
T stages			0.008
T1 + T2	1.000	Ref.	
T3 + T4	3.225	1.547–6.035	
N stages			0.001
N0	1.000	Ref.	
N + [b]	3.987	1.836–8.148	
a: Mucinous adenocarcinoma, signet ring cell carcinoma and small cell carcinoma. b: N_1、N_2、N_3			

Three cell lines including MGC-803, SGC-7901 and HGC-27 were used to evaluate the level of mRNA expression of Apelin in different GC cells *in vitro*. The results of RT-PCR analysis indicated that different cell lines presented varying Apelin expression levels, and a statistically significant difference was observed between each two groups ($P < 0.05$, Fig. 2.1). MGC-803 cells (Ct = 1.000 ± 0.344) exhibited the lowest Apelin expression levels, which represented approximately a 30-fold lower expression than in HGC-27 cells (Ct = 29.755 ± 5.067).

Western blotting was performed to assess the expression of Apelin at the protein level in MGC-803, SGC-7901 and HGC-27 cell lines. The lysates of MGC-803 cells had the lowest levels of immunoreactive Apelin based on the results of mRNA expression of Apelin. A significant difference was observed between the two groups ($P < 0.05$).

ELISA was performed to detect the concentration of cellular secretion of Apelin that was secreted by the examined cell lines into the culture medium. The results were similar to those observed in the protein and mRNA expressions of Apelin, accounting for the lowest concentration in MGC-803 cells (132.00 ± 31.97 pg/mL). In addition, a statistically significant difference was observed between each two cell lines ($P < 0.05$, Fig. 2.3).

The human Apelin expression vector, pcDNA3.1-Apelin vector was successfully transfected into MGC-803 cells, which were selected because they contain the lowest amounts of Apelin. Analyses revealed that the levels of Apelin mRNA, Apelin-encoding protein and the concentration of Apelin protein secreted in the culture medium considerably were increased in stably transfected MGC-803 cells compared to cells transfected with an empty vector (control). Moreover, the changes in Apelin expression levels exhibited a significant difference after transfection with pcDNA3.1-Apelin (Fig. 2.4, 2.5 and 2.6).

Cells were incubated with different concentrations of Apelin-13 for 24 hours, and the MTT assay subsequently performed to evaluate the effect of exogenous Apelin-13 on proliferation of MGC-803 cells. Exogenous Apelin-13 significantly ameliorated cell proliferation rate in a concentration-dependent manner, and the optimum concentration was 2.5 μmol/L (Fig. 2.7). The proliferation of MGC-803 cells that were treated with Apelin-13 (concentration of 2.5 μmol/L) for 48 hours exhibited a time-dependent relationship, presenting a significant and steady increase from 12 hours to 48 hours compared to the control group (Fig. 2.8).

The proliferation rate of MGC-803 cells transfected with Apelin-encoding pcDNA3.1-Apelin vector and incubated for 48 hours increased remarkably from 24 hours to 48 hours compared to cells transfected with empty vectors (control), with the absorbance detected at 570 nm by MTT analysis at different time intervals (Fig. 2.9)

Four types of cells were selected based on the results obtained from MTT assay as our experimental objects to evaluate migration and invasion abilities of MGC-803 cells, including untreated cells, Apelin-13 induced cells (incubated with a concentration of 2.5 μmol/L for 24 hours), mock-vector transfected cells (incubated for 24 hours after transfection with pcDNA3.1 vector) and pcDNA3.1-Apelin transfected cells (incubated for 24 hours after transfection with pcDNA3.1-Apelin vector). Apelin-13 induced cells exhibited a significant improvement on the capacity to transfer to the membranes compared to untreated cells (t=-9.577, P = 0.001) (Fig. 2.10). A similar observation was also made between mock transfected cells and cells transfected with pcDNA3.1-Apelin (t=-5.142, P = 0.007).

The rate of apoptosis induced by SAHA was substantially increased in treated cells compared to the untreated cells (control) ((15.100 ± 3.997) % vs (7.300 ± 1.745) %, $P < 0.05$) (Fig. 2.11). Strikingly, the

proportion of apoptotic cells ((14.000 ± 3.899) %) treated with both SAHA and Apelin-13, and the ratio of apoptotic cells ((14.425 ± 4.393) %) treated with both SAHA and pcNDA3.1-Apelin exhibited similar apoptotic ratios in the subgroups treated with SAHA. There was no significant correlation observed in groups treated with SAHA and SAHA + Apelin-13, SAHA and SAHA + pcNDA3.1-Apelin, respectively (t = 0.342, P = 0.774; t = 0.816, P = 0.446).

Cytokines were assessed using western blot assays to explore the underlying molecular mechanisms of Apelin-13 induction including pERK1/2, pAkt, cyclin D1 and MMP-9, and Apelin overexpression that are associated with biological behavior of MGC-803 cells. As previously mentioned, there were four subgroups, untreated cells, Apelin-13 induced cells (incubated with a concentration of 2.5 μmol/L Apelin for 24 hours), mock-vector transfected cells (incubated for 24 hours after transfection with pcDNA3.1 vector) and pcDNA3.1-Apelin transfected cells (incubated for 24 hours after transfection with pcDNA3.1-Apelin vector). By contrast, no significant correlation was observed in the protein levels of pAkt between the control and treated groups (P > 0.05), but the protein levels of other three cytokines, namely pERK1/2, cyclin D1 and MMP-9, were significantly increased relative to control cells after Apelin-13-induction and transfection with pcDNA3.1-Apelin (P < 0.05, Fig. 2.12).

We successfully established pLV-puro-Apelin and pLV-puro stable transformants through lentiviral mediation and puromycin screening with 100% transfection efficiency, namely pLV-puro-Apelin and pLV-puro. Real time RT-PCR analyses indicated that the mRNA expression level of Apelin increased considerably after transfecting pLV-puro-Apelin into MGC-803 cells compared to the control group (t=-4.236, P = 0.013, Fig. 3.1). Western blot analysis revealed that Apelin-encoding protein expression level was substantially enhanced by treatment with pLV-puro-Apelin transfected into MGC-803 cells in comparison to the control group *(*t=-3.833, P = 0.019) (Fig. 3.2).

We established a total of 14 gastric cancer xenografts formed in nude mice by subcutaneously injecting mice with MGC-803 cells transfected with pLV-puro-Apelin or MGC-803 cells transfected with pLV-puro. One nude mouse died three days after receiving a subcutaneous injection of MGC-803 cells transfected with pLV-puro-Apelin, and tumorigenesis was not observed in one nude mouse in the control group. The nude mice in the Apelin-overexpression group gradually exhibited decreased activity and poor nutritional status after injection, and the observation was terminated at 24 days after injection. Variables including (a) long diameter, (b) short diameter, and (c) weights of tumor of the nude mice were monitored twice a week by the same investigator. Furthermore, the tumor volumes (mm^3) were calculated using the formula, $V = ab^2/2$ and a tumor growth curve plotted. The neoplastic growth velocity in mice subcutaneously injected with pLV-puro-Apelin significantly increased from the fourteenth day (Fig. 3.3 and Table 3.1). A maximum body weight and tumor size of 2.96 ± 0.61 g was observed in the mice injected with MGC-803 cells of overexpressed-Apelin, whereas a minimum body weight and tumor size of 1.70 ± 0.43 g was observed in mice of the control group (Fig. 3.4). The results revealed the function of Apelin in promoting proliferation of gastric cancer cells via *in vitro* and *in vivo* experiments.

Table 3.1
The volume of gastric cancer xenografts in nude mice and statistical analysis

Time(day)	Control(± s)	Overexpression of Apelin(± s)	*t* value	*P* value
7	22.656 ± 8.702	26.775 ± 11.745	-0.630	0.543
10	61.517 ± 23.151	80.836 ± 26.352	-1.232	0.246
14	106.115 ± 36.515	196.010 ± 66.854	-2.639	0.025
17	306.789 ± 105.315	567.346 ± 198.854	-2.598	0.027
21	748.919 ± 214.059	1399.063 ± 499.872	-2.673	0.023
24	1367.348 ± 444.701	2557.645 ± 684.409	-3.261	0.009

MVD assay by CD34 immunolabeling was performed to explore the mechanism underlying the differences in neoplastic growth velocity between over-expressed Apelin and control, and to establish the relationship between Apelin overexpression and angiogenesis. MVD was significantly higher in xenograft tumors with Apelin overexpression (168.833 ± 35.078) than in the control group, which had low MVD (112.333 ± 29.859; t=-2.734, P = 0.021) (Fig. 3.5).

Discussion

Local recurrence and metastasis of tumors are the principal factors associated with poor prognosis, and are modulated by various genes and cytokines [21, 22]. The demonstrated relationship between tumorous proliferation, metastasis, recurrence and angiogenesis has prompted the discovery of various factors associated with angiogenesis to date. VEGF signaling pathway has been the center of attention in relation to tumor angiogenesis, and VEGF-targeted therapy has provided insights into the treatment of certain cancers such as lung and colon cancers [23, 24]. In addition, previous studies have revealed that VEGF signaling pathway has a significant role in tumorigenesis and development of GC, and that high VEGF expression indicated a poor prognosis [23–25]. However, the clinical benefits of adding anti-VEGF drug in human GC have not been satisfactory [25]. Therefore, it is necessary to find a novel biomarker and new antivascular targets as therapeutic targets for GC.

Apelin is an emerging endogenous ligand, which has attracted the attention of researchers because of its role in angiogenesis [9, 13, 14, 26]. Previous studies have revealed that Apelin expression is up-regulated in various human solid tumors [13, 26]. However, few studies have been conducted on the role of Apelin expression in tumorigenesis and development of human gastric cancer. In the present study, we investigated the correlation between the level of Apelin expression and clinicopathological parameters in patients with GC from our center. Mortality was significantly higher in patients with high Apelin-positive expression than in patients with low Apelin expression. In addition to high VEGF-positive expression observed in tumor tissues, this study revealed a significant positive correlation between Apelin expression and VEGF expression, which indicated the function of Apelin in angiogenesis in human GC. Nevertheless,

further studies are required to investigate whether there is a synergy between Apelin and VEFG in relation to angiogenetic effect. Feng and his colleagues demonstrated that Apelin in tumor tissues rather than serum Apelin was associated with clinicopathological features, and it was an independent prognostic factor [27]. Although Apelin was not an independent prognostic factor in this study, multivariate Cox regression analysis revealed that patients with high Apelin-positive expression exhibited a considerably poor prognosis compared to patients with low Apelin-positive expression based on previous other studies. In this study, the correlations between high Apelin-positive expression and late-staged T status, N stage, and the high incidence of vessel invasion implies that Apelin can promote local tumor recurrence and lymph node metastasis.

The mRNA levels of Apelin expression, proteins and lysates in cell culture media of three types of GC cell lines, HGC-27, MGC-803 and SGC-7901 were analyzed using RT-PCR, western blotting and ELISA to elucidate the effects and mechanisms of Apelin on biological behavior *in vitro*. Results of the present study indicated that Apelin expression in MGC-803 cells was not only low at the mRNA level but also at protein level and cellular secretion. With reference to human colon adenocarcinomas, a study by Picault demonstrated that Apelin presents varying expression levels at mRNA and protein levels in several cell lines [28]. Moreover, a similar observation was made in human non-small lung cancer [15]. MGC-803 cell line is characterized by poor differentiation, whereas HGC-27 cell line is an undifferentiated cell and SGC-7901 cell line can spread metastatically. The different features of previously mentioned cells could be associated with the varying levels of Apelin expression.

The MGC-803 cell line was used in this study. Apelin was over-expressed in cell lines transfected with pcDNA3.1-Apelin, which was confirmed by RT-PCR, western blot and ELISA analyses. The results suggested that Apelin secreted by cancer cells can function through paracrine and autocrine mechanisms. Furthermore, results indicated that both Apelin overexpression and exogenous Apelin remarkably ameliorated proliferation and migration of MGC-803 cells. Previous studies have revealed that exogenous Apelin can enhance cell proliferation and migration, such as in human lung adenocarcinomas cell A549 [29] and human prostate cancer cell LNCaP [30]. Moreover, Apelin is resistant to tumor cell apoptosis in hepatocellular carcinoma cell HepG2 [16] and vascular smooth muscle cell VSMCs [31]. However, a few studies have revealed that neither exogenous Apelin nor overexpression of Apelin could promote human colorectal cancer cell proliferation, but xenograft tumors transfected with cells overexpressing Apelin could promote tumor growth in mice [28].

SAHA, a member of histone deacetylase inhibitor, can induce apoptosis in MGC-803 cells according to a previous study [20]. To our knowledge, the relationship between overexpression of Apelin and malignant biological behavior in human GC cells both *in vitro* and *in vivo* has not been studied. Remarkably, SAHA did not affect the apoptotic ability of MGC-803 cell lines transfected with pcDNA3.1-Apelin or treated with exogenous Apelin when compared to the control group in this study.

According to studies conducted in the recent past, both mitogen-activated protein kinase kinase/(MAPK)/ERK and phosphoinositide 3-kinase (PI3K)/Akt signaling pathways have a critical role in

the proliferation, migration, angiogenesis and inhibition of apoptosis in tumor cells, including the human GC cells [32, 33]. Tumor cells promote ERK phosphorylation, thereby resulting in transcription of cyclin D1 that largely stimulates tumorous growth in the ERK signaling pathway. Cyclin D1 promotes cell cycle transition from G1 to S phase and exerts mitogenic effects on cell proliferation [34]. Both the MAPK/ERK and PI3K/Akt signaling pathways participate in tumor invasion primarily by up-regulating MMP-9 transcription, which has been reported to be associated with cancer invasion and metastasis [35, 36]. The anti-apoptotic properties were reflected in the MAPK/ERK and PI3K/Akt signaling pathways through stimulation of the expression of anti-apoptotic peptide belonging to Bcl-2 family or inhibition of a caspase-mediated pathway.

The results obtained from our analysis demonstrated that the protein expression levels of ERK phosphorylation (pERK) signaling pathway, cyclin D1 that is associated with cell proliferation and MMP-9 involved in invasion were increased by both overexpression of Apelin and exogenous Apelin in comparison to the control group. Strikingly, there was no significant difference in the expression of Akt phosphorylation (pAkt) between the treatment and control groups. According to a study by Picault and his colleagues, Apelin/APJ signaling pathway suppressed apoptosis through phosphorylation of Apelin [28]. MG132 is a proteasome inhibitor, which performs a crucial role in the activation of apoptosis by downregulating pAkt in multiple tumorous cell lines through an intrinsic pathway [37]. Studies have indicated that Apelin/APJ induces Akt phosphorylation to counteract apoptosis activated by MG132 in human colorectal LoVo cells [28]. Remarkably, exogenous Apelin neither improved the expression of pERK nor increased proliferation rate in LoVo cells [28]. Yang *et al*. reported that Apelin-13 induced cell proliferation and promoted autophagy through phosphorylation of ERK, subsequently activating the downstream transduction cascades in human lung cancer cell line A549 [29]. Moreover, exogenous Apelin induces phosphorylation of ERK and Akt, resulting in cell migration and inhibition of apoptosis rather than cell proliferation in human lymphatic endothelial cells [31].

The results of the present study corresponded to the findings of most previous studies, implying that Apelin can stimulate proliferation of tumor cells. Conversely, anti-apoptotic effect of Apelin that is activated by SAHA and Akt phosphorylation *in vitro* was not observed. There might be an anfractuosity relationship between SAHA and the MAPK/ERK and PI3K/Akt signaling pathways. This suggested that Apelin modulated apoptosis signaling by participating in the MAPK/ERK signaling pathway in human GC cells. Therefore, further studies should be conducted to investigate if there is a negative correlation between Apelin and SAHA. Notably, a positive feedback between Apelin expression and ERK activation was observed. Nevertheless, we failed to down-regulate Apelin expression levels in human GC cell line HGC-27 due to lack of an effective SiRNA molecular marker, but we are trying to apply other approaches to delete the Apelin gene.

To the best of our knowledge, this is the first study to establish human GC cell xenograft models with overexpressed Apelin. The findings of the present study suggest that Apelin overexpression promotes growth of human GC cells and angiogenesis *in vivo* when compared with the control group. Apelin has been characterized as a novel angiogenic factor, which can stimulate vascular endothelial cell

proliferation and migration through extrinsic and intrinsic pathways. In addition, knocking down Apelin or APJ can efficiently block angiogenesis [38]. Sorli *et al*. revealed that Apelin overexpression increased the formation of tumorous vessels and accelerated tumor growth, in addition to the paracrine role in tumor neoangiogenesis [39]. Kidoya *et al*. demonstrated that the Apelin/APJ signaling pathway induced maturation of tumor vascular morphology and function [40]. MVD is the gold standard for estimating tumor angiogenesis, which is closely associated with tumor invasion and metastasis, and is an independent prognosis factor [39]. Berta *et al*. observed that Apelin overexpression could significantly stimulate tumor growth, increase MVD and capillary perimeter [15]. Muto *et al*. demonstrated that Apelin-13 antagonist could block tumor proliferation or angiogenic activity in hepatocellular carcinoma xenograft model, which confirmed the role of Apelin overexpression in tumourigenesis through angiogenesis [41]. A common observation made among the mentioned studies including the present study was that implantation of tumor cells transfected with overexpressed Apelin increased tumor growth in nude mice and simultaneously enhanced the expression of MVD in comparison with the control group.

Conclusion

Overall, Apelin was highly expressed in human gastric cancer tissues compared to adjacent normal tissues. The expression level of Apelin was associated with vessel invasion, N stage, T stage, VEGF and MVD expressions. In addition, the high expression of Apelin is positively correlated with late-stage T status, lymph node metastasis, and vessel invasion resulting in poor prognosis. Overexpressed or exogenous Apelin promotes proliferation and invasion of MGC-803 cell lines by activating ERK/Cyclin D1/MMP-9 signaling pathway, but does not inhibit apoptosis induced by SAHA in MGC-803 cell lines. Overexpressed Apelin enhances angiogenesis resulting in the growth of subcutaneous xenograft *in vivo*. The occurrence and development of cancers are closely linked with angiogenesis and proliferation, thus Apelin antagonist can be a novel therapeutic target for human GC.

Abbreviations

Gastric cancer (Gc), real-time reverse transcription-polymerase chain reaction (RT-PCR), vascular endothelial growth factor (VEGF), computed tomography (CT), intensive modulation radiotherapy (IMRT), progression-free survival (PFS), Overall survival (OS), sodium dodecyl sulfate (SDS), Microvessel densities (MVD), polyvinylidene fluoride (PVDF), Tris-buffered saline (TBS), horseradish peroxidase (HRP), dimethyl sulfoxide (DMSO), Suberoylanilide hydroxamic acid (SAHA), histone deacetylase inhibitor (HDACI), mitogen-activated protein kinase kinase/(MAPK), phosphoinositide 3-kinase (PI3K).

Declarations

Ethics approval and consent to participate

All procedures performed in study involving human participants were in accordance with the ethical standards of the institutional and national research committee and with the 1964 Helsinki declaration

and its later amendments or comparable ethical standards.

Consent for publication

Informed consent was obtained from all individual.

Availability of data and materials

The datasets used or analyzed during the current study were available from the corresponding author on reasonable request.

Competing interests

None of the authors have any conflicts of interest.

Funding

This work was not supported by any research fund.

Authors' contributions

LJT: Conceptualization, Methodology, Formal analysis and Writing - Original Draft; HZL: Software, Formal analysis and Data Curation; QZ: Investigation and Resources. DZG: Validation. JY: Visualization. HTG: Formal analysis; YJZ: Investigation; YQH: Project administration; YZH: Writing - Review & Editing and Supervision. All authors agreed to be accountable for all aspects of the work.

Acknowledgements

We thank all participants and patients who participated in this study.

References

1. Torre LA, Bray F, Siegel RL, et al. Global cancer statistics, 2012. CA Cancer J Clin. 2015;65:87–108.
2. Ferlay J, Soerjomataram I, Dikshit R, et al. Cancer incidence and mortality worldwide: sources, methods and major patterns in GLOBOCAN 2012. Int J Cancer. 2015;136:E359–86.
3. Msika S, Tazi MA, Benhamiche AM, et al. Population-based study of diagnosis, treatment and prognosis of gastric cancer. Br J Surg. 1997;84:1474–8.
4. Zhang XF, Huang CM, Lu HS, et al. Surgical treatment and prognosis of gastric cancer in 2,613 patients. World J Gastroenterol. 2004;10:3405–8.
5. Shen W, Li J, Cui J, et al. [Meta-analysis of prognosis after surgical treatment in gastric cancer patients with liver metastasis]. Zhonghua Wei Chang Wai Ke Za Zhi. 2014;17:128–32.
6. Bian Y, Wang Z, Xu J, et al. Elevated Rictor expression is associated with tumor progression and poor prognosis in patients with gastric cancer. Biochem Biophys Res Commun. 2015;464:534–40.

7. Liu H, Zhang Y, Hao X, et al. GPRC5A overexpression predicted advanced biological behaviors and poor prognosis in patients with gastric cancer. Tumour Biol. 2016;37:503–10.
8. Tatemoto K, Hosoya M, Habata Y, et al. Isolation and characterization of a novel endogenous peptide ligand for the human APJ receptor. Biochem Biophys Res Commun. 1998;251:471–6.
9. Claesson-Welsh L. What is normal? Apelin and VEGFA, drivers of tumor vessel abnormality. EMBO Mol Med. 2019;11:e10892.
10. Chen MM, Ashley EA, Deng DX, et al. Novel role for the potent endogenous inotrope Apelin in human cardiac dysfunction. Circulation. 2003;108:1432–9.
11. Kowanetz M, Ferrara N. Vascular endothelial growth factor signaling pathways: therapeutic perspective. Clin Cancer Res. 2006;12:5018–22.
12. Waldner MJ, Wirtz S, Jefremow A, et al. VEGF receptor signaling links inflammation and tumorigenesis in colitis-associated cancer. J Exp Med. 2010;207:2855–68.
13. Sorli SC, Le Gonidec S, Knibiehler B, Audigier Y. Apelin is a potent activator of tumour neoangiogenesis. Oncogene. 2007;26:7692–9.
14. Sorli SC, van den Berghe L, Masri B, et al. Therapeutic potential of interfering with Apelin signalling. Drug Discov Today. 2006;11:1100–6.
15. Berta J, Kenessey I, Dobos J, et al. Apelin expression in human non-small cell lung cancer: role in angiogenesis and prognosis. J Thorac Oncol. 2010;5:1120–9.
16. Heo K, Kim YH, Sung HJ, et al. Hypoxia-induced up-regulation of Apelin is associated with a poor prognosis in oral squamous cell carcinoma patients. Oral Oncol. 2012;48:500–6.
17. Tovari J, Gilly R, Raso E, et al. Recombinant human erythropoietin alpha targets intratumoral blood vessels, improving chemotherapy in human xenograft models. Cancer Res. 2005;65:7186–93.
18. Livak KJ, Schmittgen TD. Analysis of relative gene expression data using real-time quantitative PCR and the 2(-Delta Delta C(T)) Method. Methods. 2001;25:402–8.
19. Masri B, Morin N, Pedebernade L, et al. The Apelin receptor is coupled to Gi1 or Gi2 protein and is differentially desensitized by Apelin fragments. J Biol Chem. 2006;281:18317–26.
20. Lu H, Yang XF, Tian XQ, et al. The in vitro and vivo anti-tumor effects and molecular mechanisms of suberoylanilide hydroxamic acid (SAHA) and MG132 on the aggressive phenotypes of gastric cancer cells. Oncotarget. 2016;7:56508–25.
21. Zang ZJ, Cutcutache I, Poon SL, et al. Exome sequencing of gastric adenocarcinoma identifies recurrent somatic mutations in cell adhesion and chromatin remodeling genes. Nat Genet. 2012;44:570–4.
22. Oltean S, Bates DO. Hallmarks of alternative splicing in cancer. Oncogene. 2014;33:5311–8.
23. Giaccone G. The potential of antiangiogenic therapy in non-small cell lung cancer. Clin Cancer Res. 2007;13:1961–70.
24. Tabernero J, Yoshino T, Cohn AL, et al. Ramucirumab versus placebo in combination with second-line FOLFIRI in patients with metastatic colorectal carcinoma that progressed during or after first-line

therapy with bevacizumab, oxaliplatin, and a fluoropyrimidine (RAISE): a randomised, double-blind, multicentre, phase 3 study. Lancet Oncol. 2015;16:499–508.

25. Van Cutsem E, de Haas S, Kang YK, et al. Bevacizumab in combination with chemotherapy as first-line therapy in advanced gastric cancer: a biomarker evaluation from the AVAGAST randomized phase III trial. J Clin Oncol. 2012;30:2119–27.
26. Amir E, Mandoky L, Blackhall F, et al. Antivascular agents for non-small-cell lung cancer: current status and future directions. Expert Opin Investig Drugs. 2009;18:1667–86.
27. Feng M, Yao G, Yu H, et al. Tumor Apelin, not serum Apelin, is associated with the clinical features and prognosis of gastric cancer. BMC Cancer. 2016;16:794.
28. Picault FX, Chaves-Almagro C, Projetti F, et al. Tumour co-expression of Apelin and its receptor is the basis of an autocrine loop involved in the growth of colon adenocarcinomas. Eur J Cancer. 2014;50:663–74.
29. Yang L, Su T, Lv D, et al. ERK1/2 mediates lung adenocarcinoma cell proliferation and autophagy induced by Apelin-13. Acta Biochim Biophys Sin (Shanghai). 2014;46:100–11.
30. Wan Y, Zeng ZC, Xi M, et al. Dysregulated microRNA-224/Apelin axis associated with aggressive progression and poor prognosis in patients with prostate cancer. Hum Pathol. 2015;46:295–303.
31. Cui RR, Mao DA, Yi L, et al. Apelin suppresses apoptosis of human vascular smooth muscle cells via APJ/PI3-K/Akt signaling pathways. Amino Acids. 2010;39:1193–200.
32. Gala K, Chandarlapaty S. Molecular pathways: HER3 targeted therapy. Clin Cancer Res. 2014;20:1410–6.
33. Shen C, Song YH, Xie Y, et al. Downregulation of HADH promotes gastric cancer progression via Akt signaling pathway. Oncotarget. 2017;8:76279–89.
34. Musgrove EA, Caldon CE, Barraclough J, et al. Cyclin D as a therapeutic target in cancer. Nat Rev Cancer. 2011;11:558–72.
35. Kang MH, Kim JS, Seo JE, et al. BMP2 accelerates the motility and invasiveness of gastric cancer cells via activation of the phosphatidylinositol 3-kinase (PI3K)/Akt pathway. Exp Cell Res. 2010;316:24–37.
36. Han J, Xie Y, Lan F, et al. Additive effects of EGF and IL-1beta regulate tumor cell migration and invasion in gastric adenocarcinoma via activation of ERK1/2. Int J Oncol. 2014;45:291–301.
37. Yu C, Friday BB, Lai JP, et al. Cytotoxic synergy between the multikinase inhibitor sorafenib and the proteasome inhibitor bortezomib in vitro: induction of apoptosis through Akt and c-Jun NH2-terminal kinase pathways. Mol Cancer Ther. 2006;5:2378–87.
38. Lv D, Li H, Chen L. Apelin and APJ, a novel critical factor and therapeutic target for atherosclerosis. Acta Biochim Biophys Sin (Shanghai). 2013;45:527–33.
39. Kalin RE, Kretz MP, Meyer AM, et al. Paracrine and autocrine mechanisms of Apelin signaling govern embryonic and tumor angiogenesis. Dev Biol. 2007;305:599–614.

40. Kidoya H, Kunii N, Naito H, et al. The Apelin/APJ system induces maturation of the tumor vasculature and improves the efficiency of immune therapy. Oncogene. 2012;31:3254–64.
41. Muto J, Shirabe K, Yoshizumi T, et al. The Apelin-APJ system induces tumor arteriogenesis in hepatocellular carcinoma. Anticancer Res. 2014;34:5313–20.

Figures

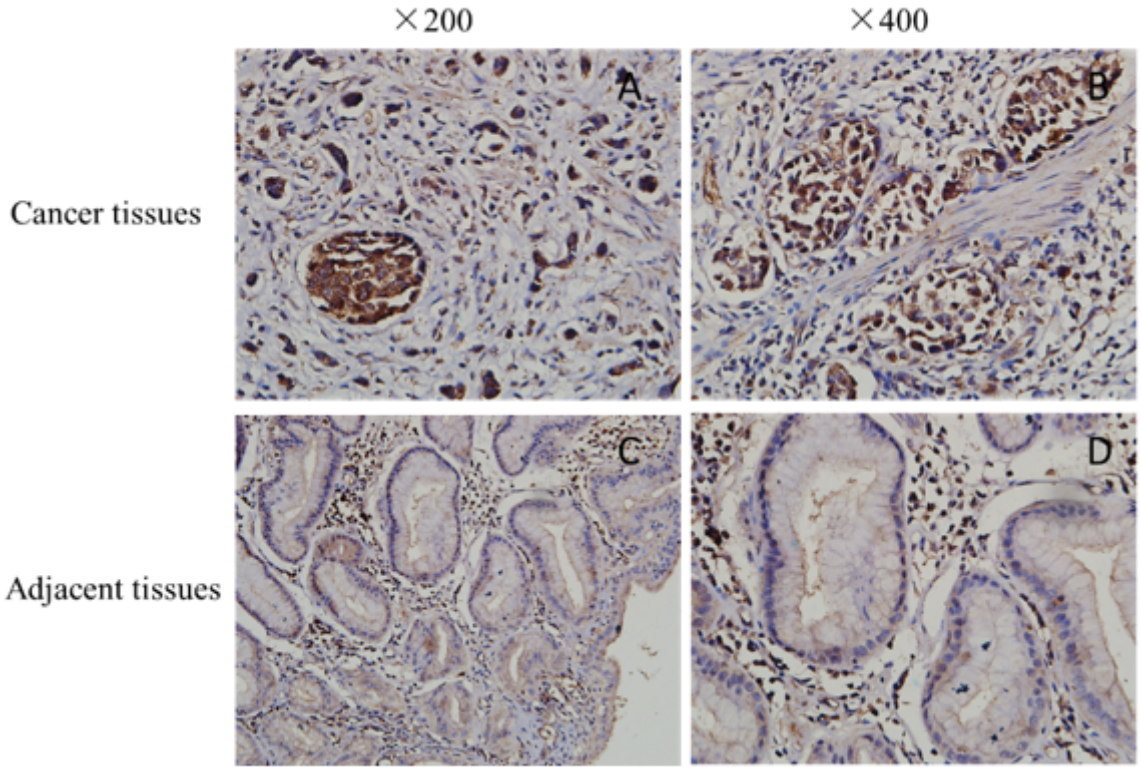

Figure 1

Immunohistochemical staining for Apelin in gastric cancer tissues (A, B) and adjacent normal tissues (C, D) (corresponding to low and high Apelin expression, respectively) Magnification, ×200(A, C), ×400(B, D).

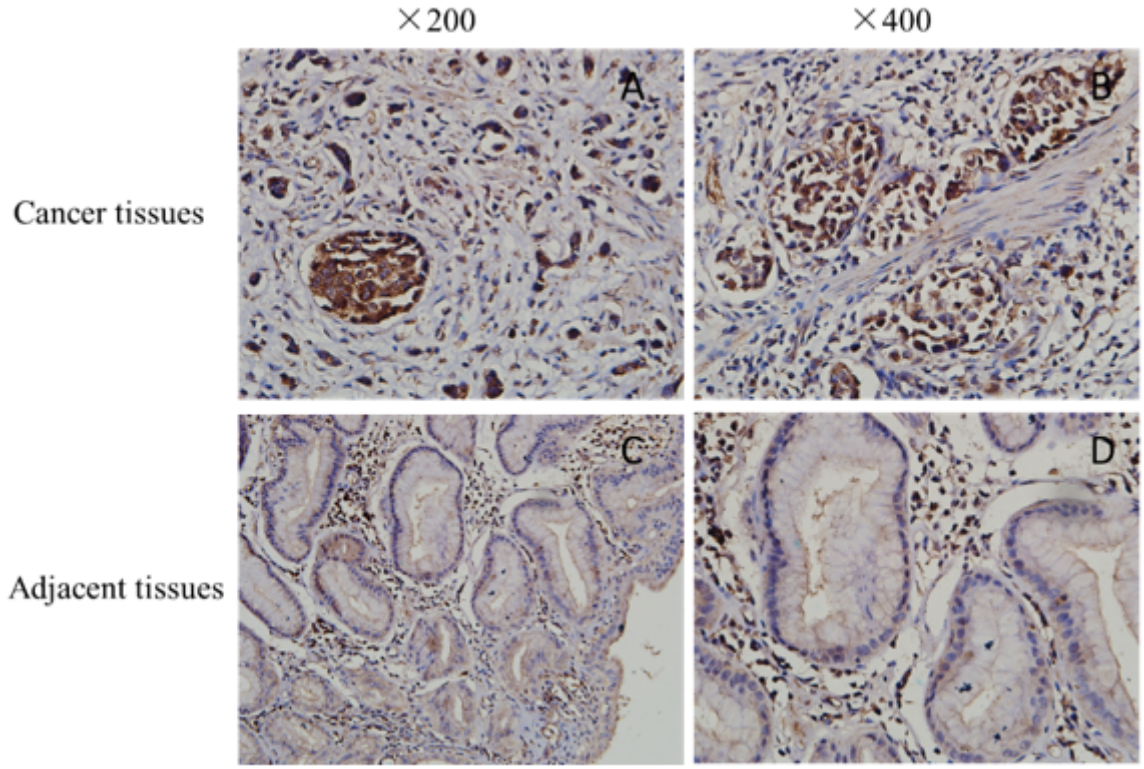

Figure 1

Immunohistochemical staining for Apelin in gastric cancer tissues (A, B) and adjacent normal tissues (C, D) (corresponding to low and high Apelin expression, respectively) Magnification, ×200(A, C), ×400(B, D).

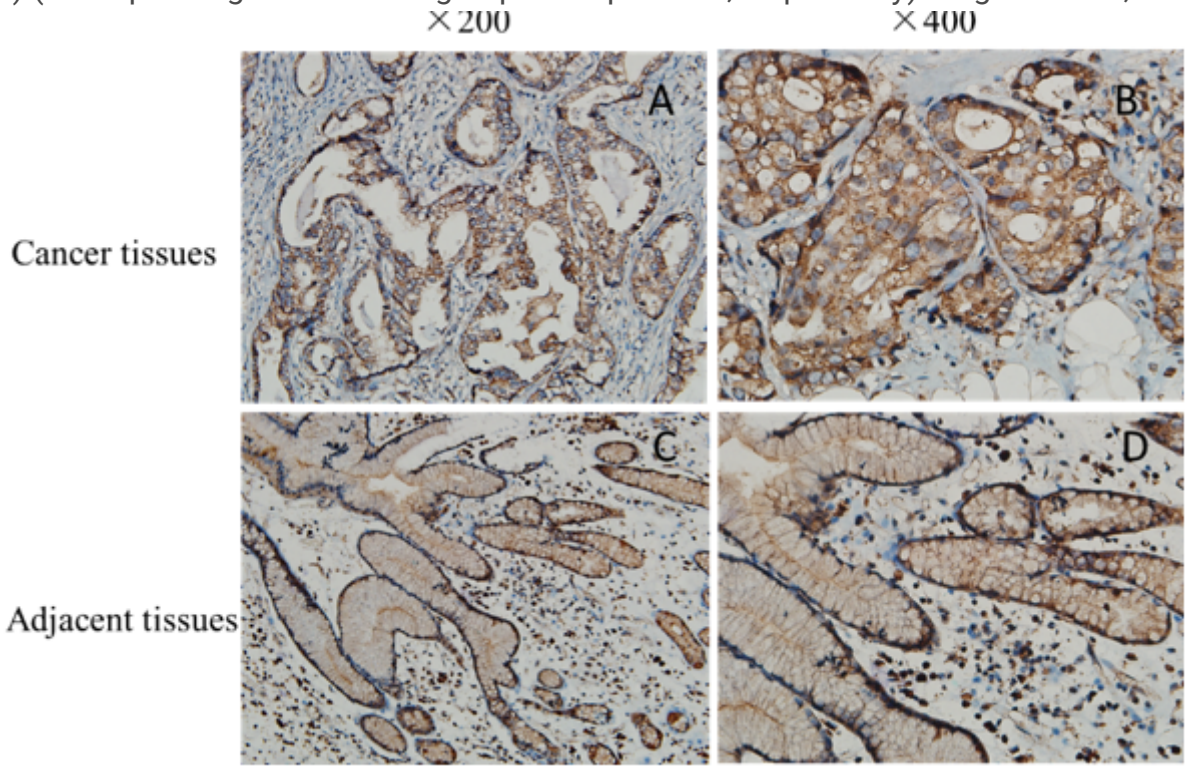

Figure 2

Immunohistochemical staining for VEGF in gastric cancer tissues (A, B) and adjacent normal tissues (C, D) (corresponding to low and high VEGF expression, respectively) Magnification, ×200(A, C), ×400(B, D).

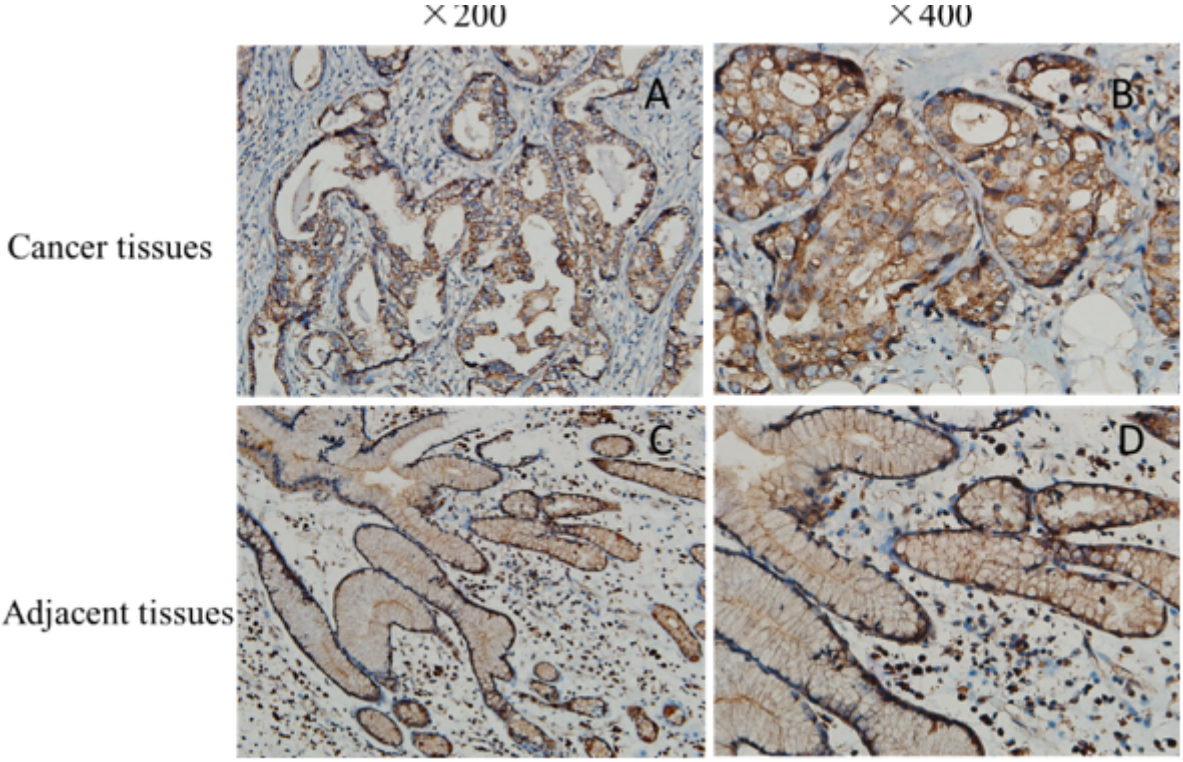

Figure 2

Immunohistochemical staining for VEGF in gastric cancer tissues (A, B) and adjacent normal tissues (C, D) (corresponding to low and high VEGF expression, respectively) Magnification, ×200(A, C), ×400(B, D).

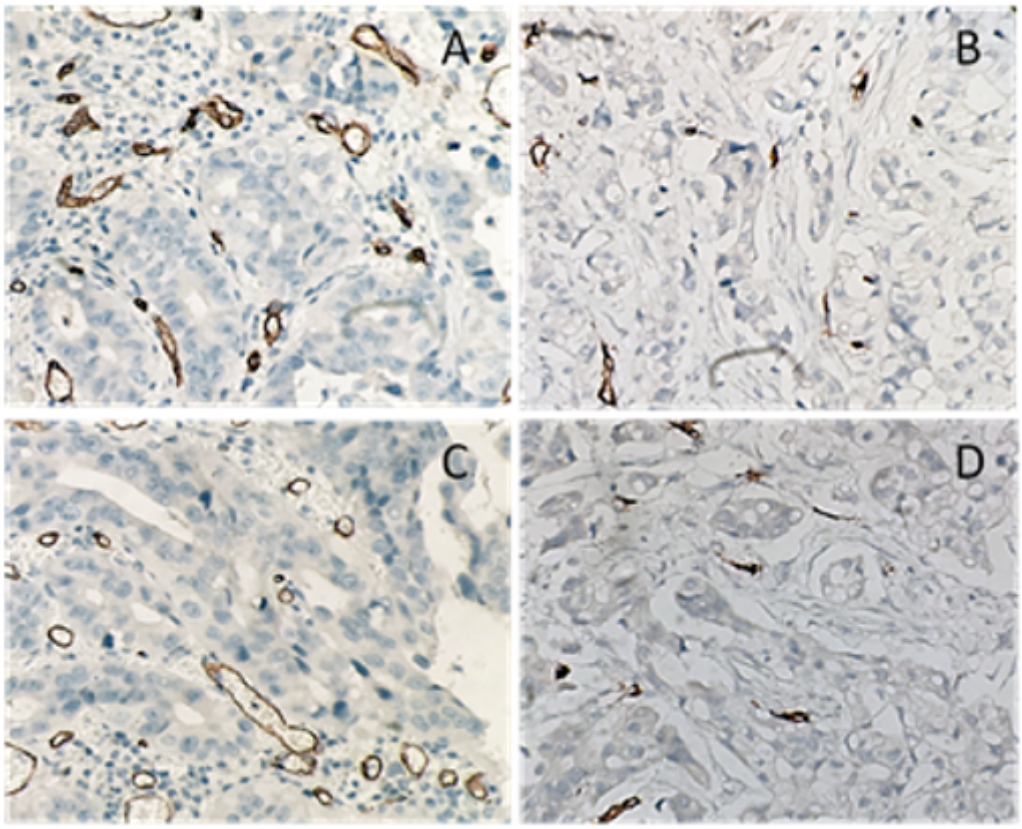

Figure 3

Immunohistochemical staining for MVD in gastric cancer tissues. A: Apelin-positive subgroup accompanied with high MVD expression; B: Apelin-negative subgroup accompanied with low MVD expression; C: VEGF-positive subgroup accompanied with high MVD expression; D: VEGF-negative subgroup accompanied with low MVD expression; Magnification×200)

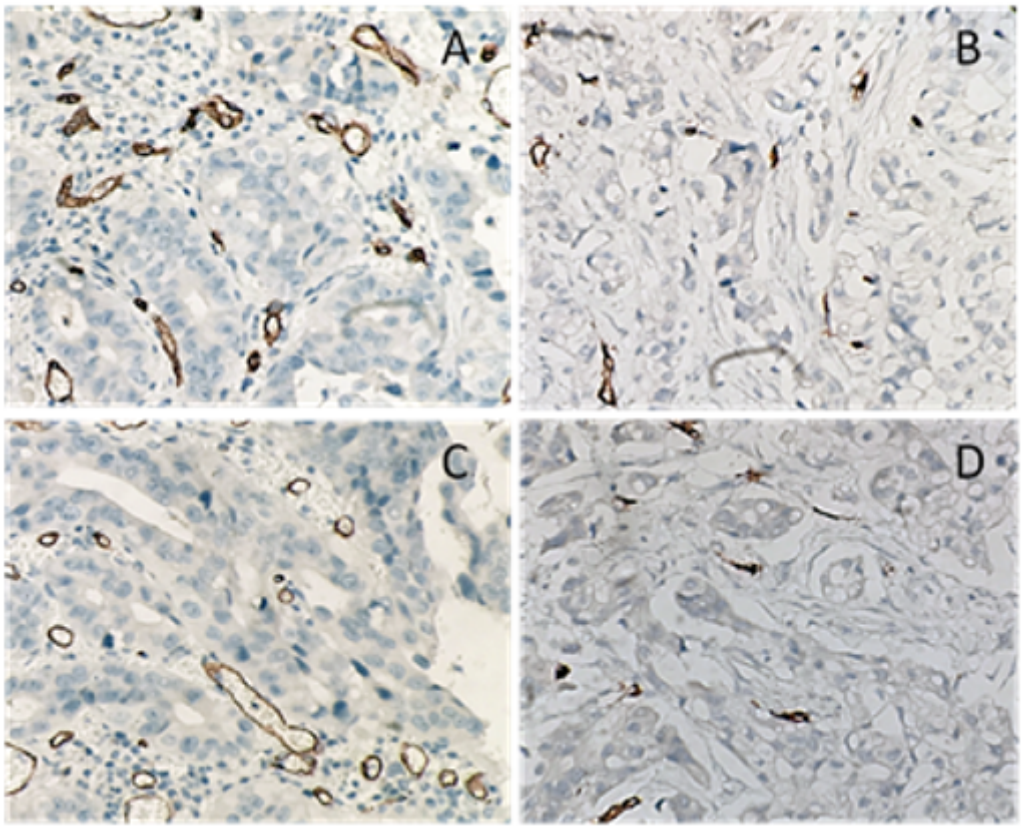

Figure 3

Immunohistochemical staining for MVD in gastric cancer tissues. A: Apelin-positive subgroup accompanied with high MVD expression; B: Apelin-negative subgroup accompanied with low MVD expression; C: VEGF-positive subgroup accompanied with high MVD expression; D: VEGF-negative subgroup accompanied with low MVD expression; Magnification×200)

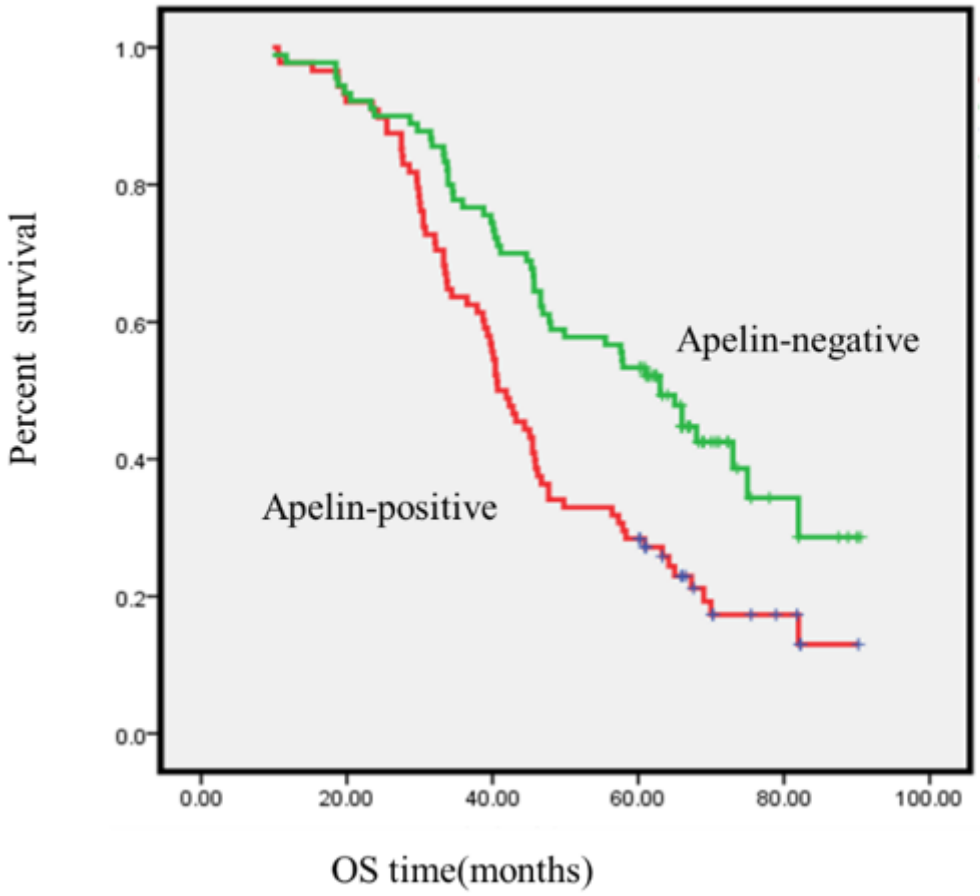

Figure 4

Kaplan-Meier curves for 178 patients diagnosed with GC in relation to Apelin expression. Patients of Apelin-negative subgroup had significantly longer OS period (60.2 months) compared with those of Apelin-negative (40.7 months).

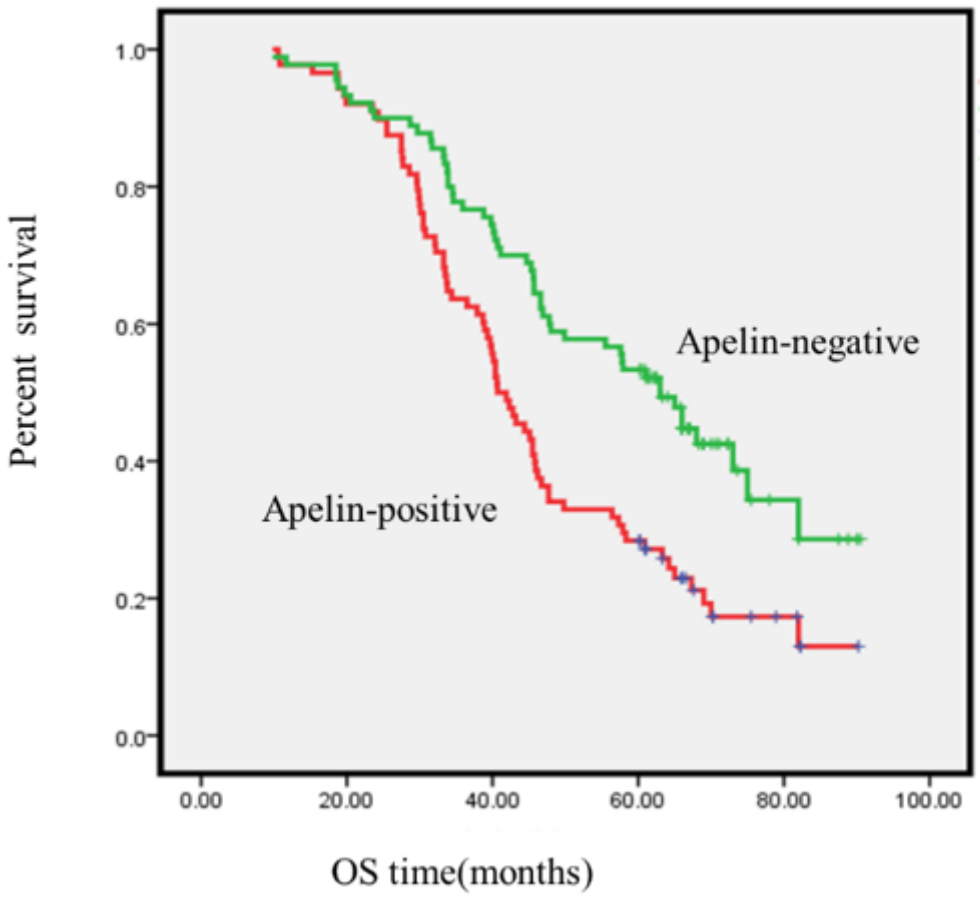

Figure 4

Kaplan-Meier curves for 178 patients diagnosed with GC in relation to Apelin expression. Patients of Apelin-negative subgroup had significantly longer OS period (60.2 months) compared with those of Apelin-negative (40.7 months).

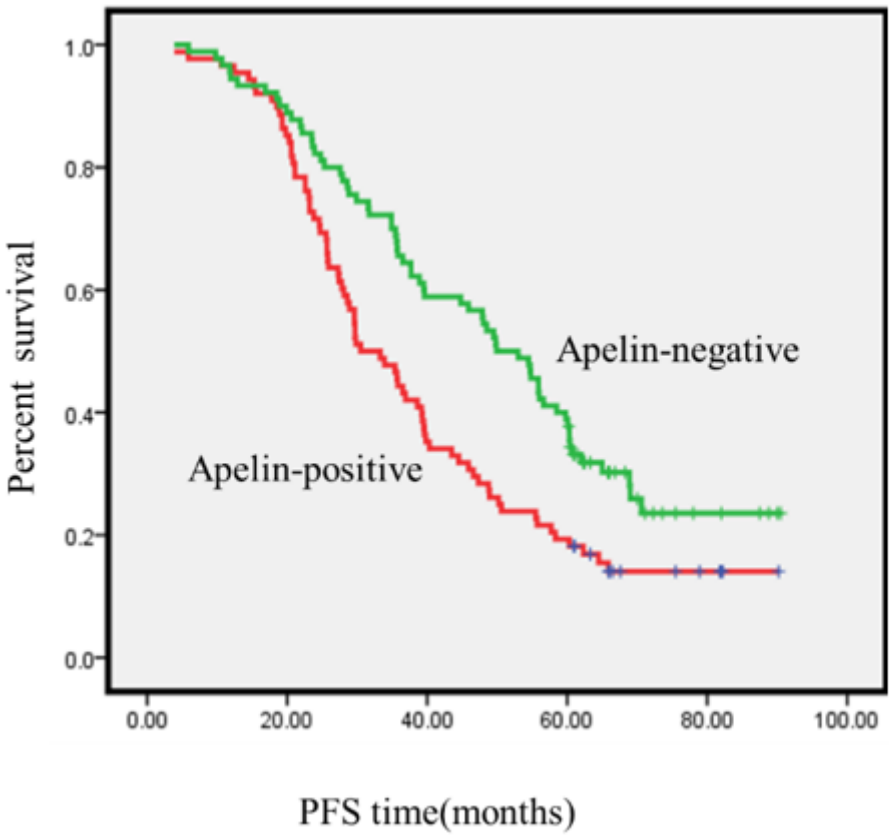

Figure 5

Kaplan-Meier curves for the PFS of 178 patients diagnosed with GC in relation to Apelin expression. Patients of Apelin-negative subgroup had significantly longer PFS period (49.8 months) compared with those of Apelin-negative (30.5 months).

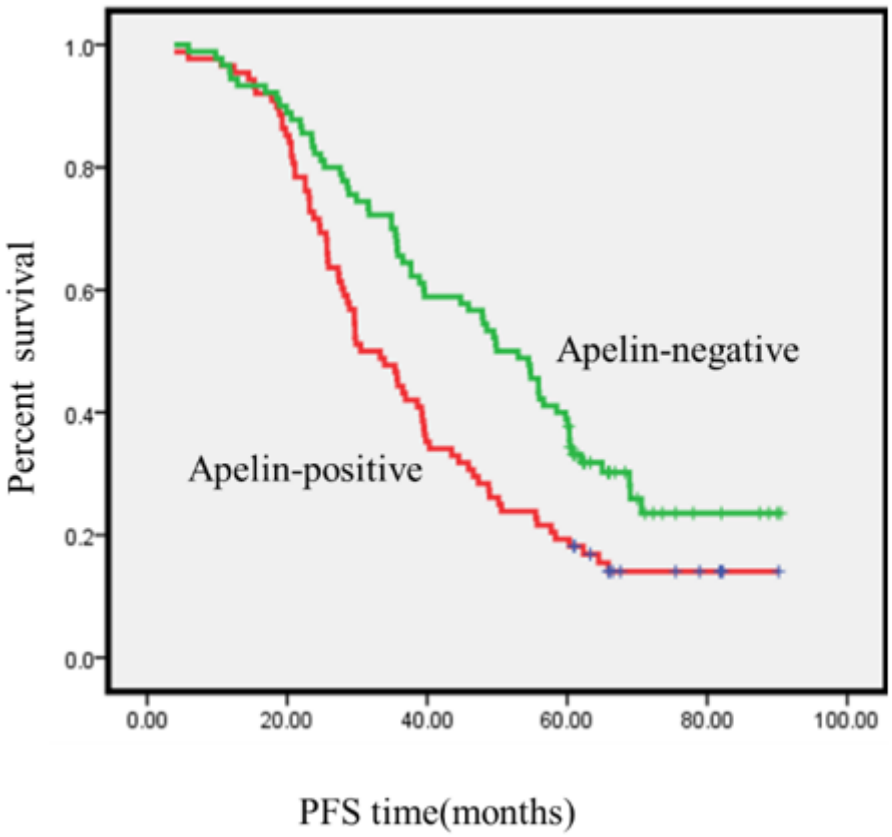

Figure 5

Kaplan-Meier curves for the PFS of 178 patients diagnosed with GC in relation to Apelin expression. Patients of Apelin-negative subgroup had significantly longer PFS period (49.8 months) compared with those of Apelin-negative (30.5 months).

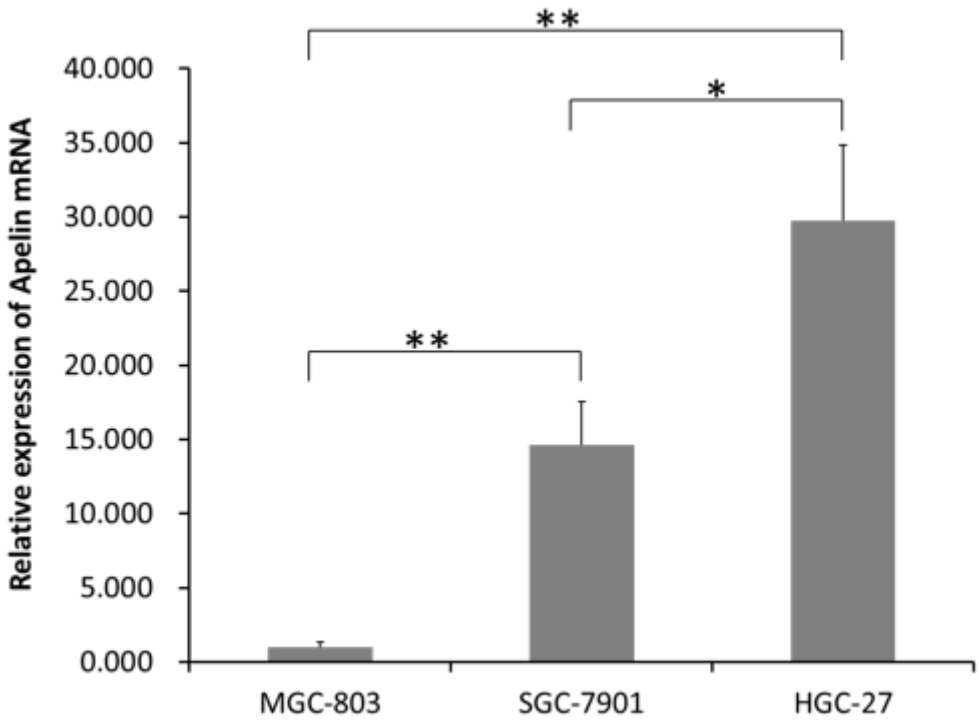

Figure 6

Expression of Apelin mRNA in different GC cell lines by RT-PCR. There was a statistical difference between two cell lines（*P＜0.05，** P＜0.01）

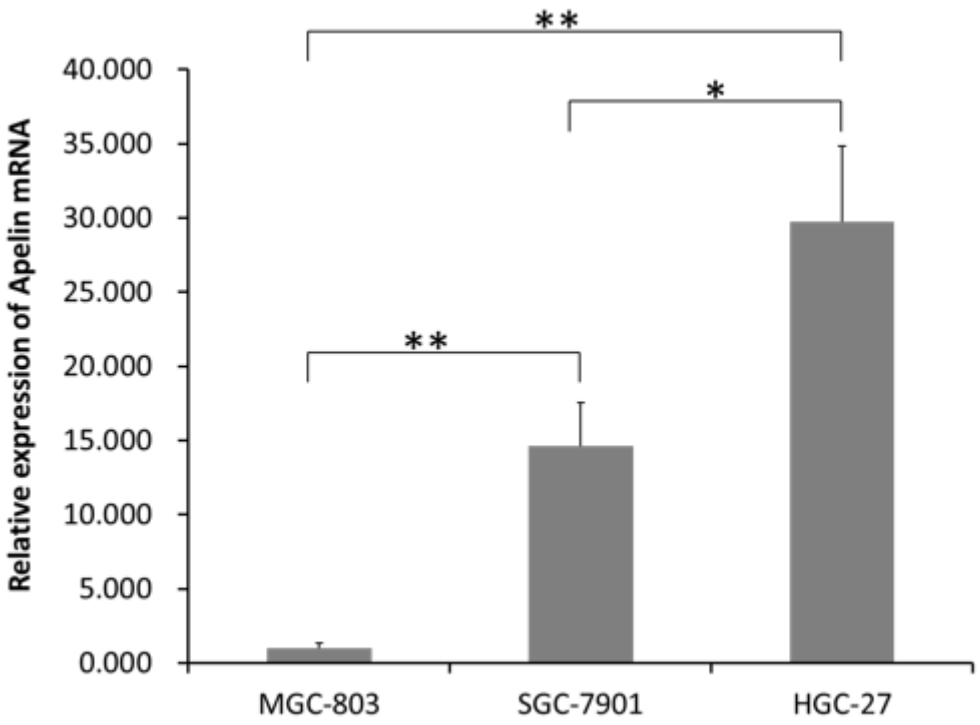

Figure 6

Expression of Apelin mRNA in different GC cell lines by RT-PCR. There was a statistical difference between two cell lines（*P＜0.05，** P＜0.01）

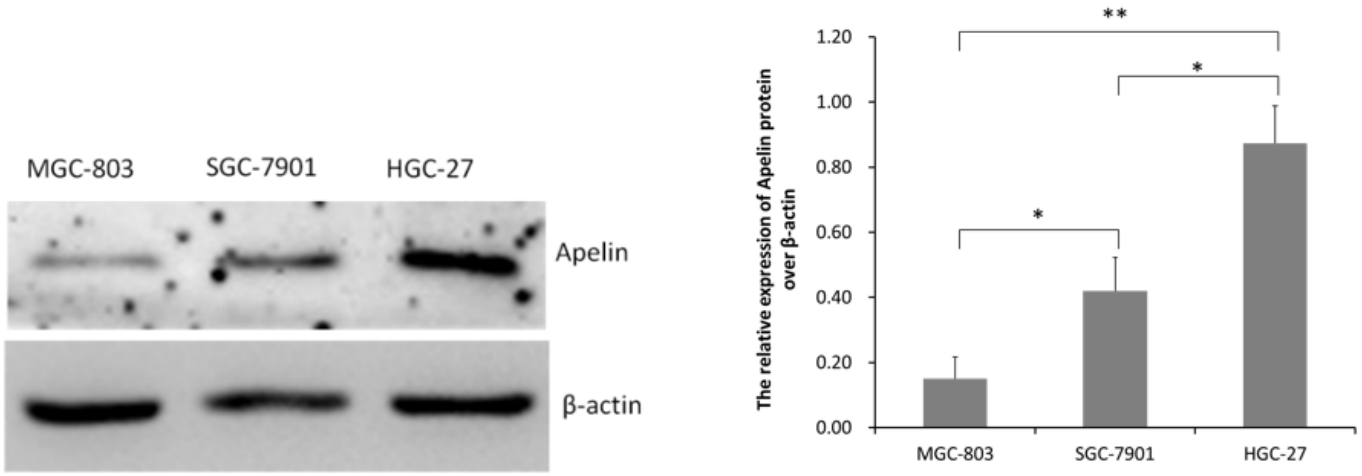

Figure 7

Expression of Apelin protein in different GC cell lines by Western blot analysis. There was a statistical difference between two cell lines（*P＜0.05，** P＜0.01）

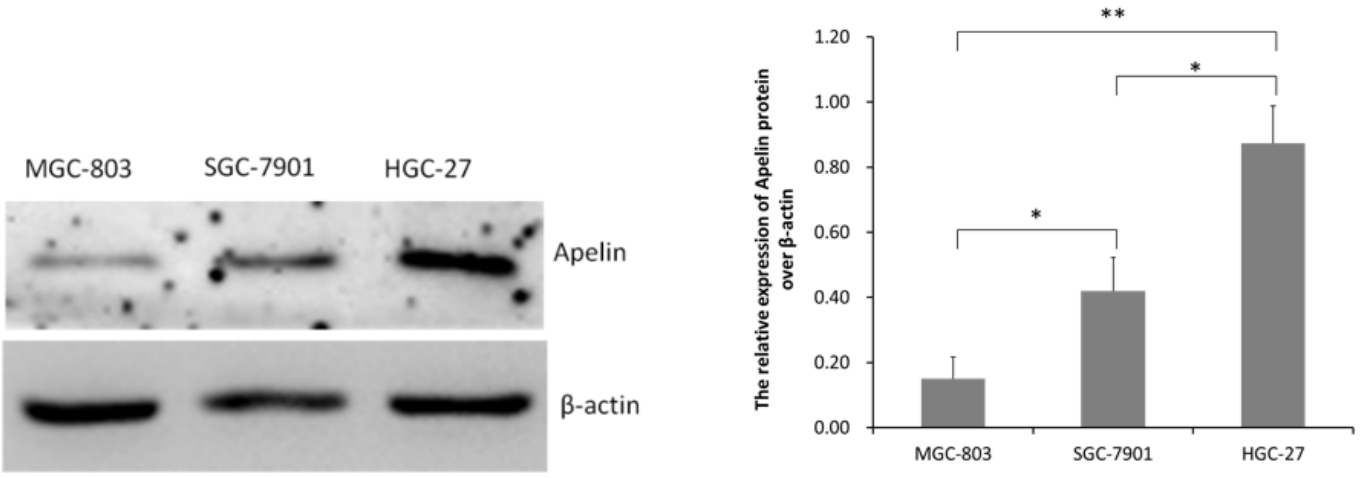

Figure 7

Expression of Apelin protein in different GC cell lines by Western blot analysis. There was a statistical difference between two cell lines（*P＜0.05；** P＜0.01）

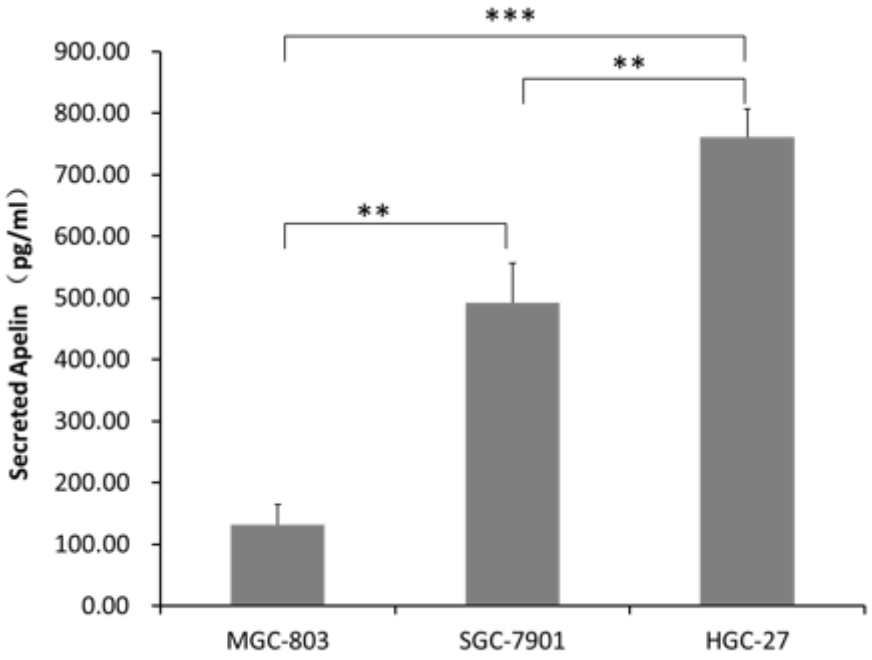

Figure 8

Levels of secreted Apelin protein in different GC cell lines verified by ELISA. There was a statistical difference between two cell lines（** P＜0.01；***P＜0.001）

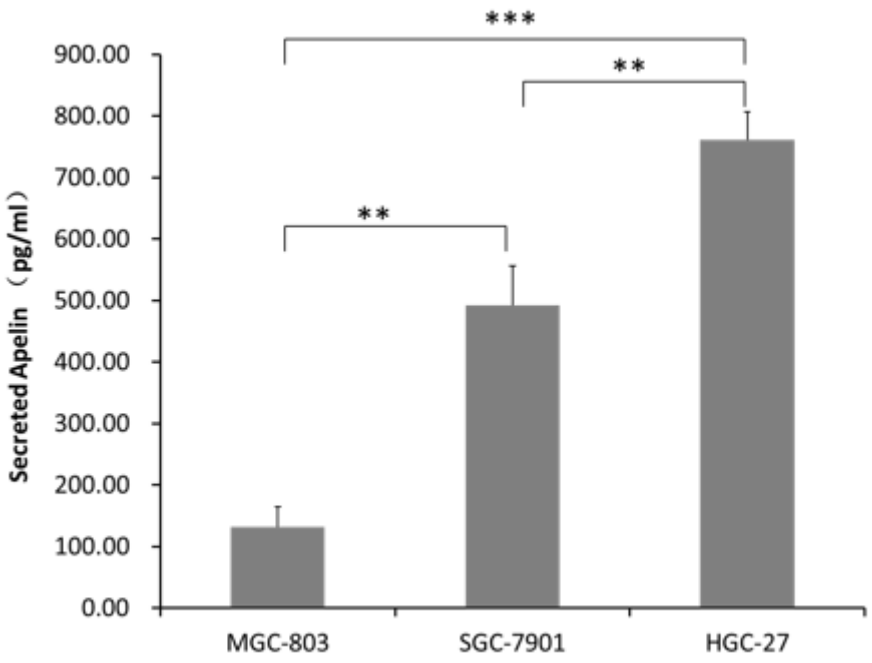

Figure 8

Levels of secreted Apelin protein in different GC cell lines verified by ELISA. There was a statistical difference between two cell lines** P0.01***P0.001

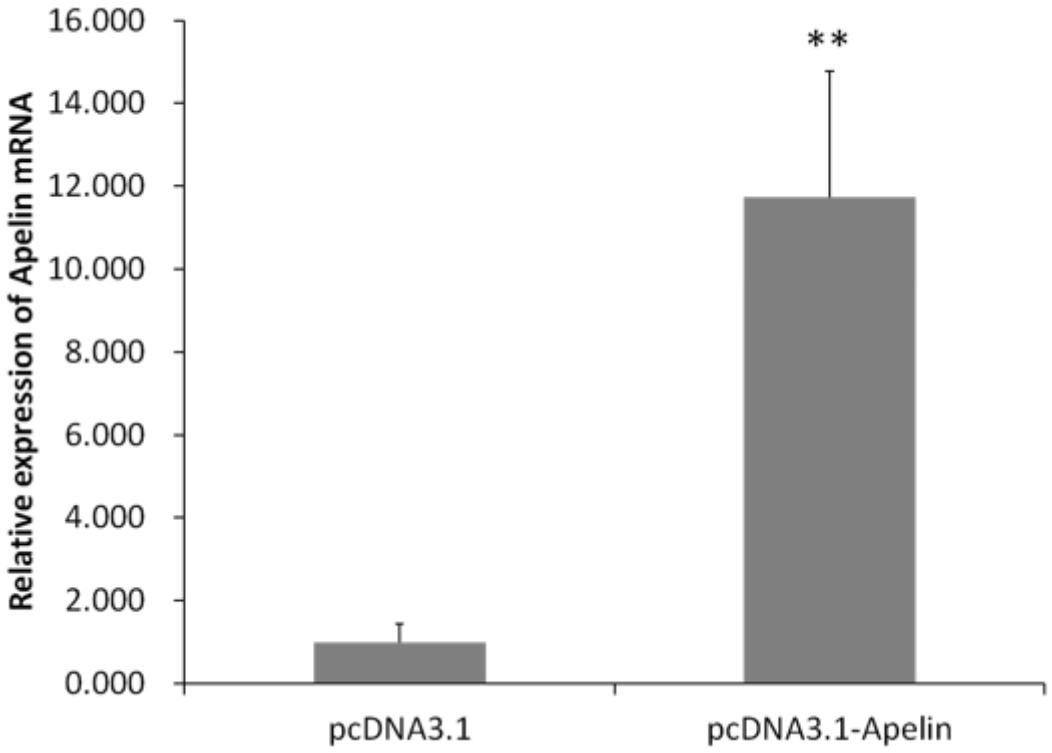

Figure 9

RT-PCR analysis of the relative expression of Apelin mRNA before and after transfection. When MGC-803 cells were transfected with pcDNA3.1-Apelin, the relative expression of Apelin was significantly elevated. (** P0.01

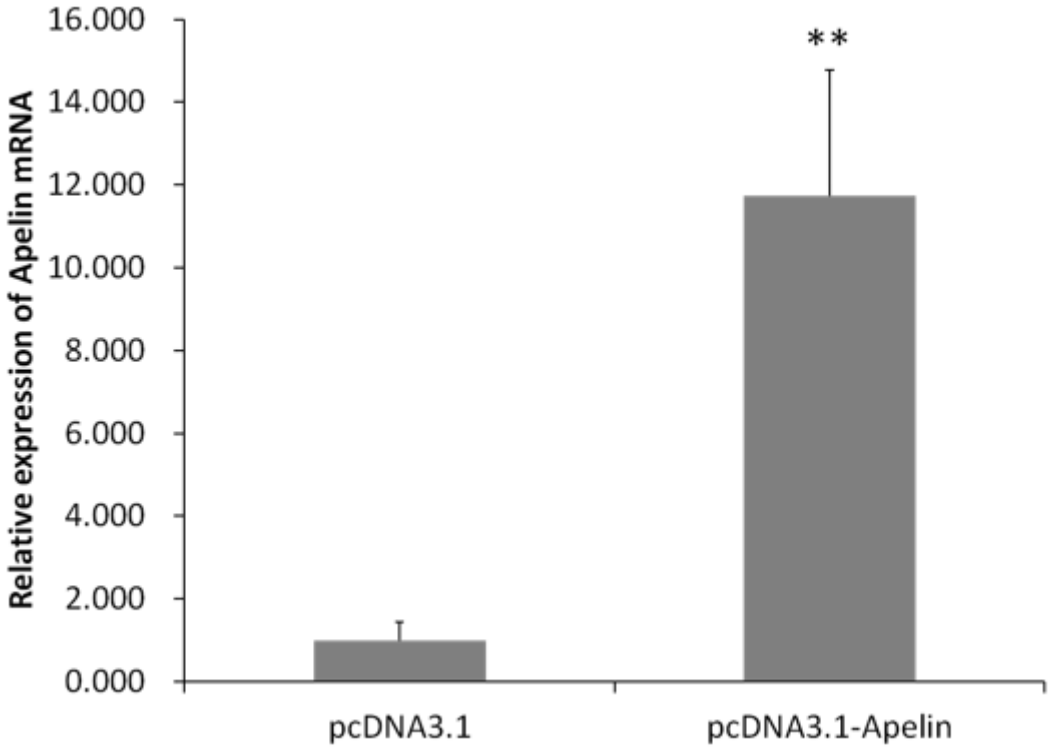

Figure 9

RT-PCR analysis of the relative expression of Apelin mRNA before and after transfection. When MGC-803 cells were transfected with pcDNA3.1-Apelin, the relative expression of Apelin was significantly elevated. (** P0.01

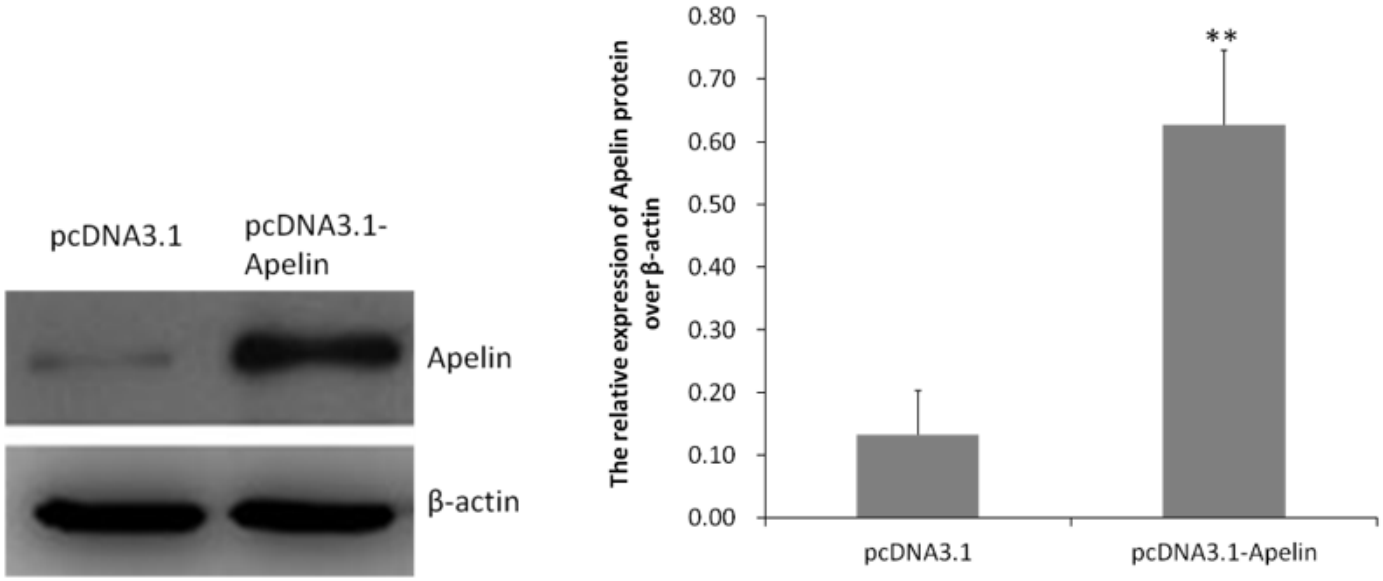

Figure 10

Western blot analysis for the expression of Apelin before and after transfection. When MGC-803 cells were transfected with pcDNA3.1-Apelin, the relative expression of Apelin protein in MGC-803 cells was significantly elevated. (**P0.01

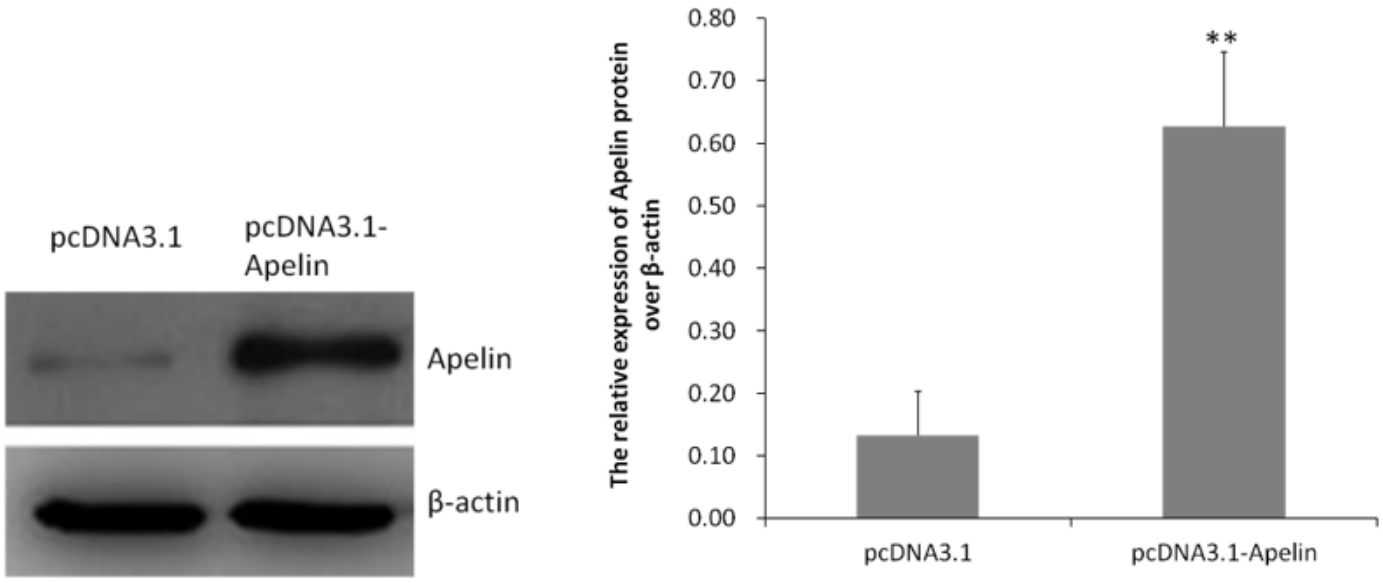

Figure 10

Western blot analysis for the expression of Apelin before and after transfection. When MGC-803 cells were transfected with pcDNA3.1-Apelin, the relative expression of Apelin protein in MGC-803 cells was significantly elevated. (**P0.01

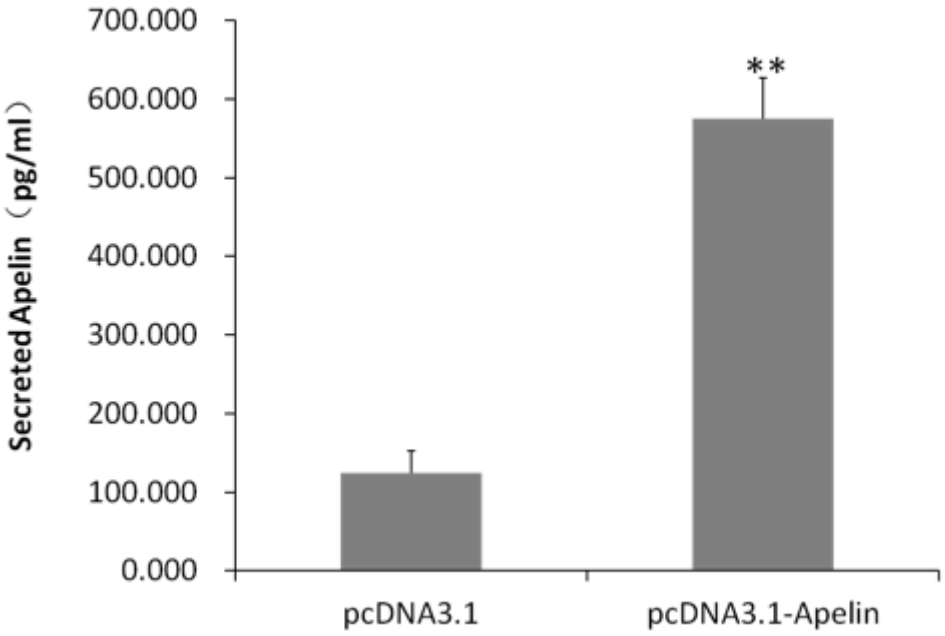

Figure 11

ELISA analysis of the expression of secreted Apelin protein before and after transfection. When MGC-803 cells were transfected with pcDNA3.1-Apelin, the relative expression of secreted Apelin in MGC-803 cells was significantly elevated（**P＜0.01）

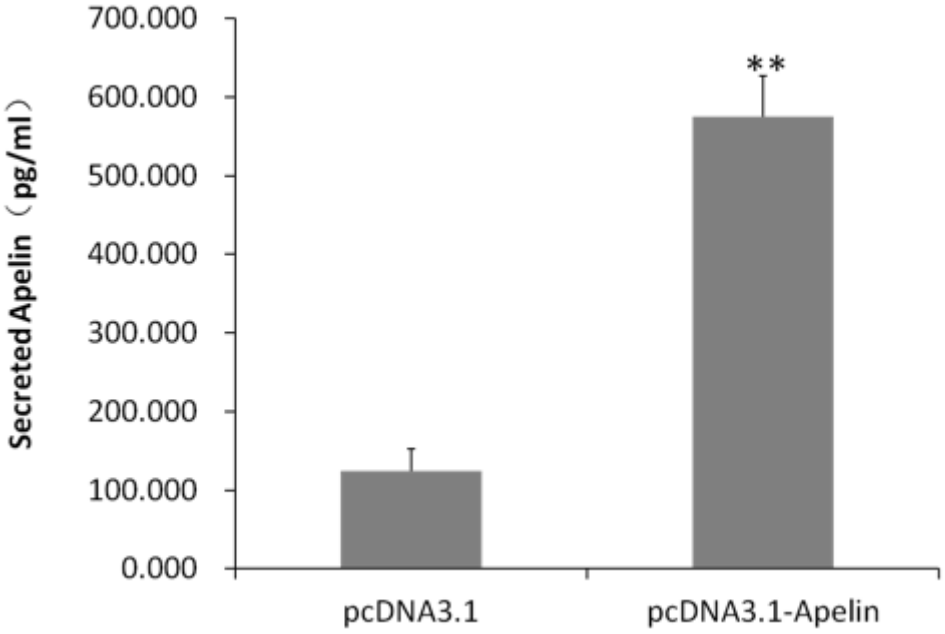

Figure 11

ELISA analysis of the expression of secreted Apelin protein before and after transfection. When MGC-803 cells were transfected with pcDNA3.1-Apelin, the relative expression of secreted Apelin in MGC-803 cells was significantly elevated（**P＜0.01）

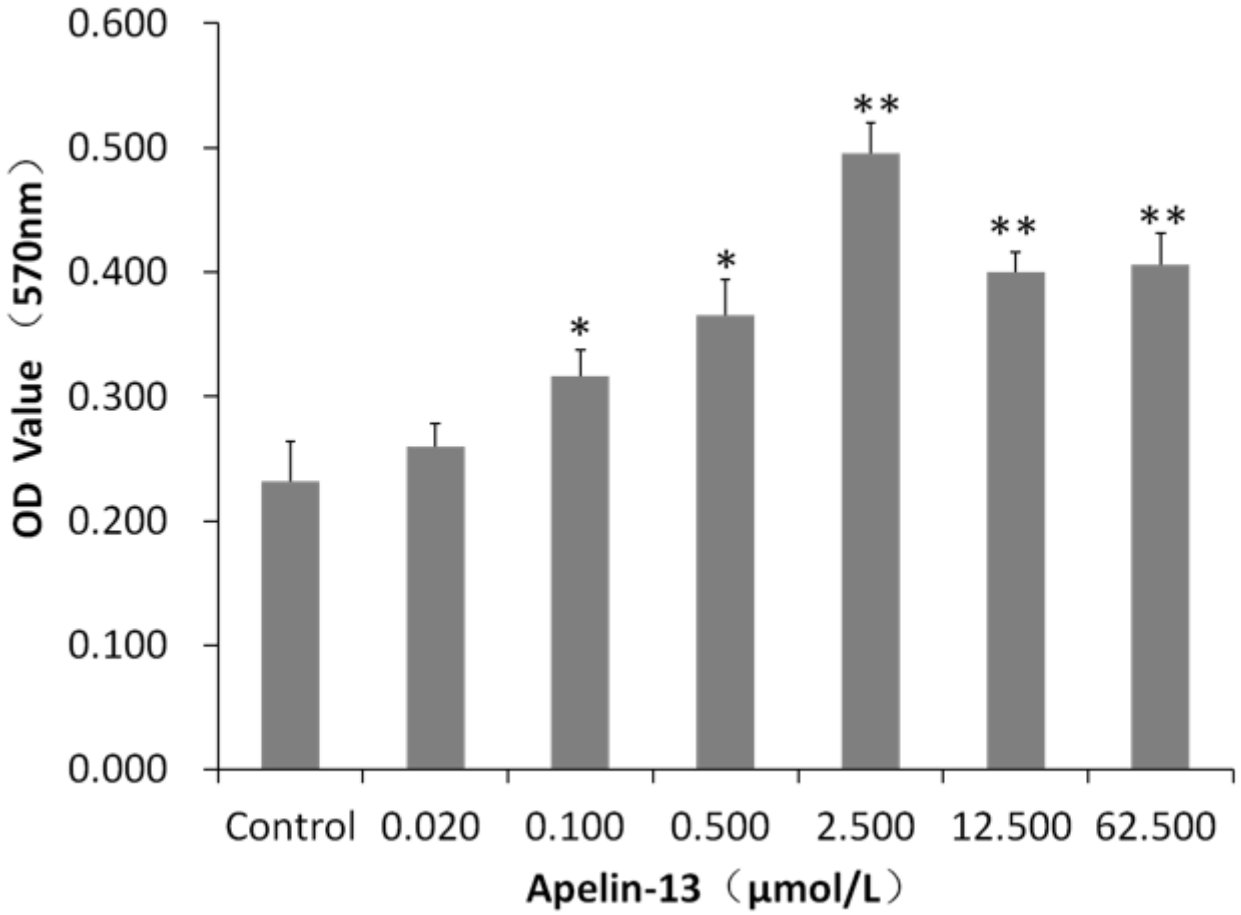

Figure 12

The proliferation of MGC-803 cells by MTT assay. Induced by different concentrations of Apelin-13 after 24 hours. (*Compared with the control group P□0.05, **Compared with the control group P□0.01)

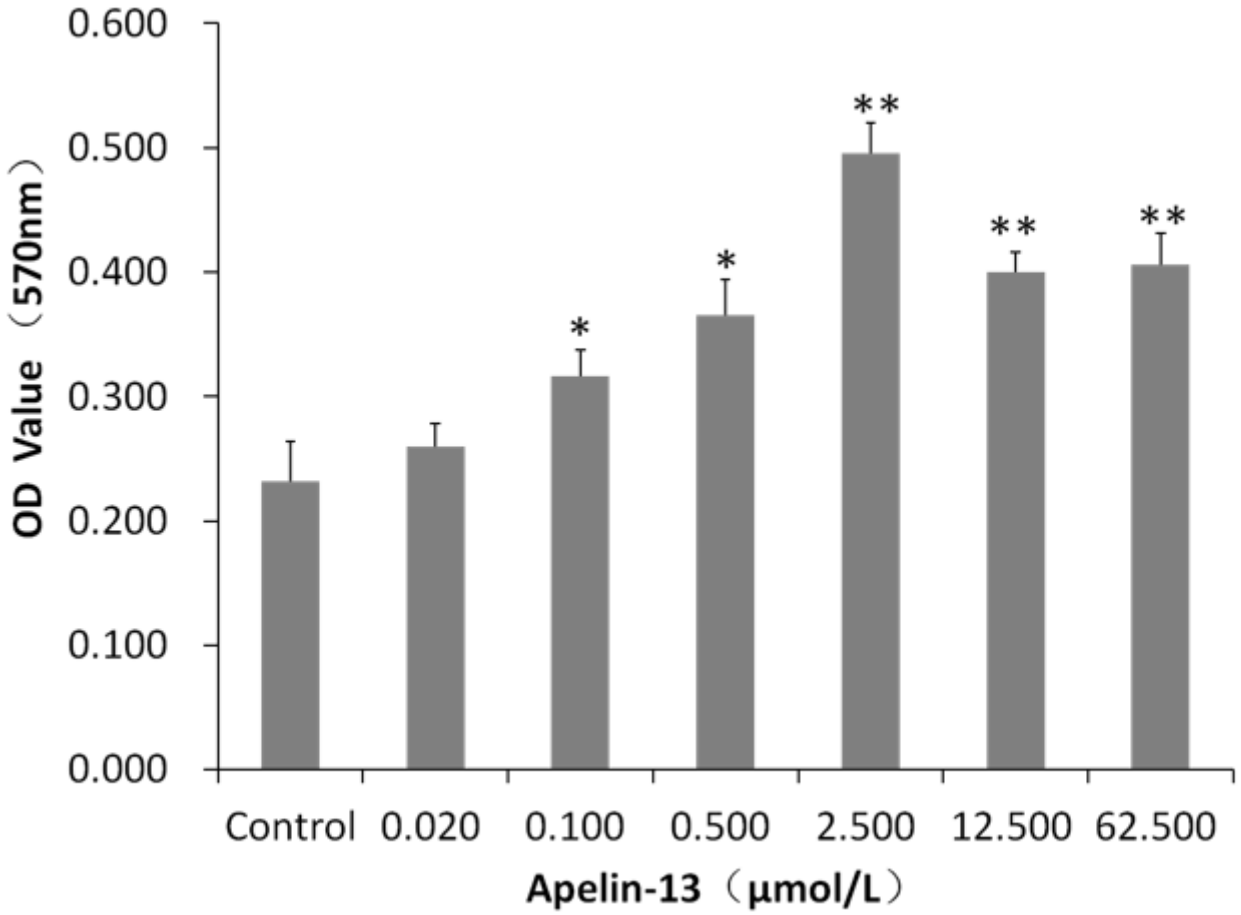

Figure 12

The proliferation of MGC-803 cells by MTT assay. Induced by different concentrations of Apelin-13 after 24 hours. (*Compared with the control group P□0.05, **Compared with the control group P□0.01)

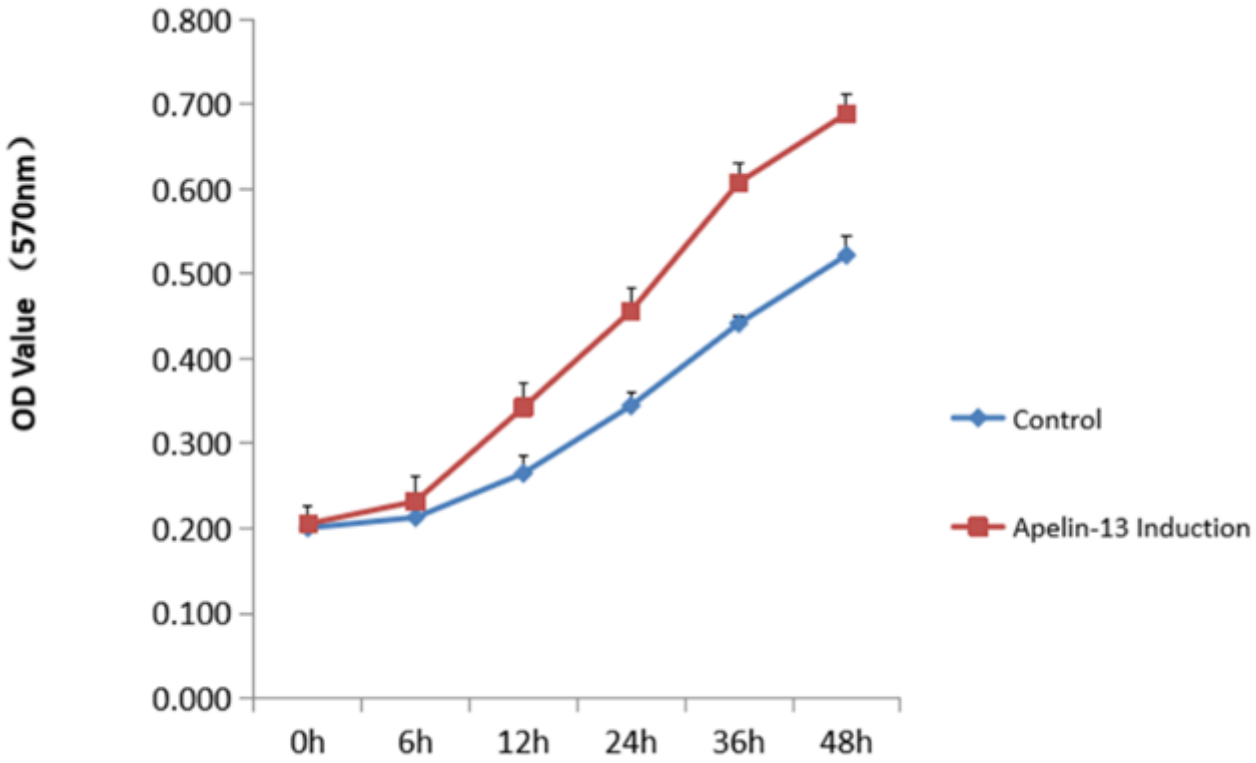

Figure 13

The proliferation of MGC-803 cells at different time points. The MGC-803 cells were induced by Apelin-13(2.5μmol/L) by MTT assay. (*Compared with the control group P□0.05, **Compared with the control group P□0.01).

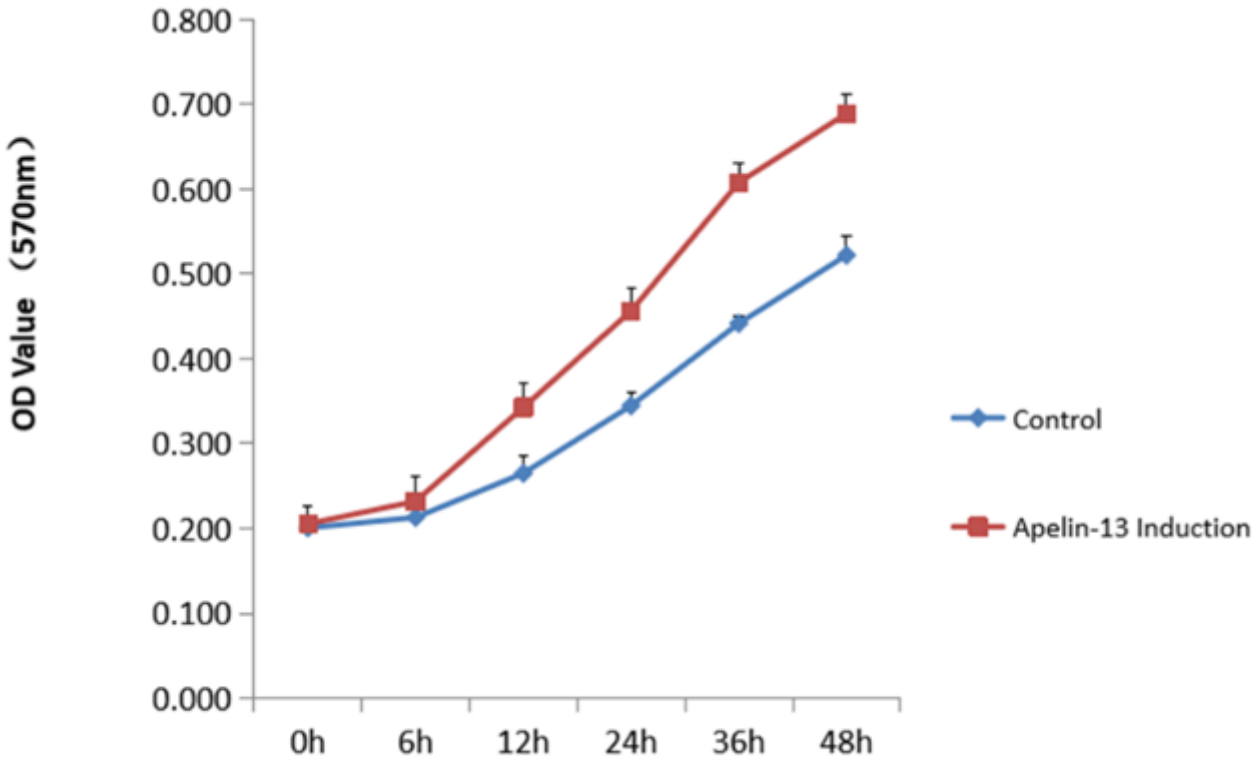

Figure 13

The proliferation of MGC-803 cells at different time points. The MGC-803 cells were induced by Apelin-13(2.5μmol/L) by MTT assay. (*Compared with the control group P□0.05, **Compared with the control group P□0.01).

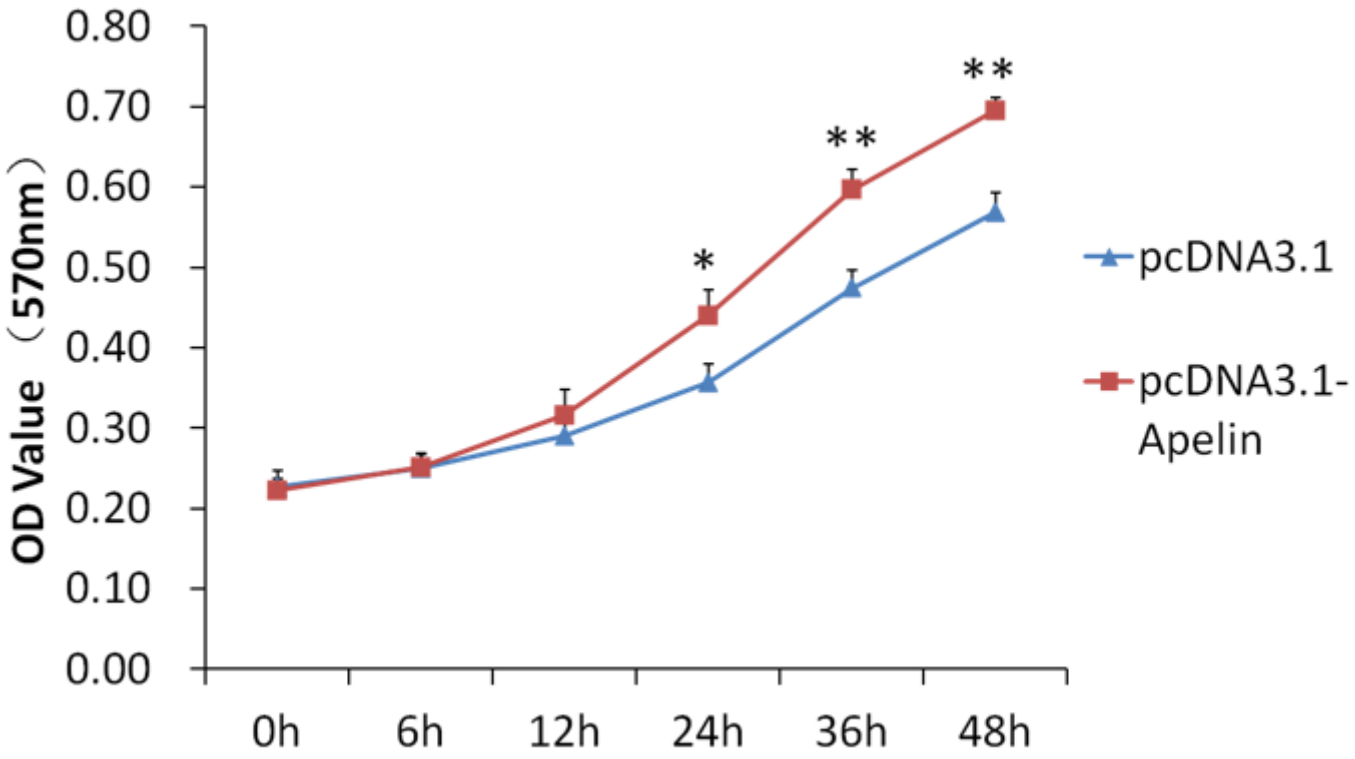

Figure 14

The proliferation after transfection by MTT assay. The proliferation of MGC-803 cells was measured transfected with pcDNA3.1-Apelin or pcDNA3.1 at different time point. (*Compared with the control group P□0.05, **Compared with the control group P□0.01).

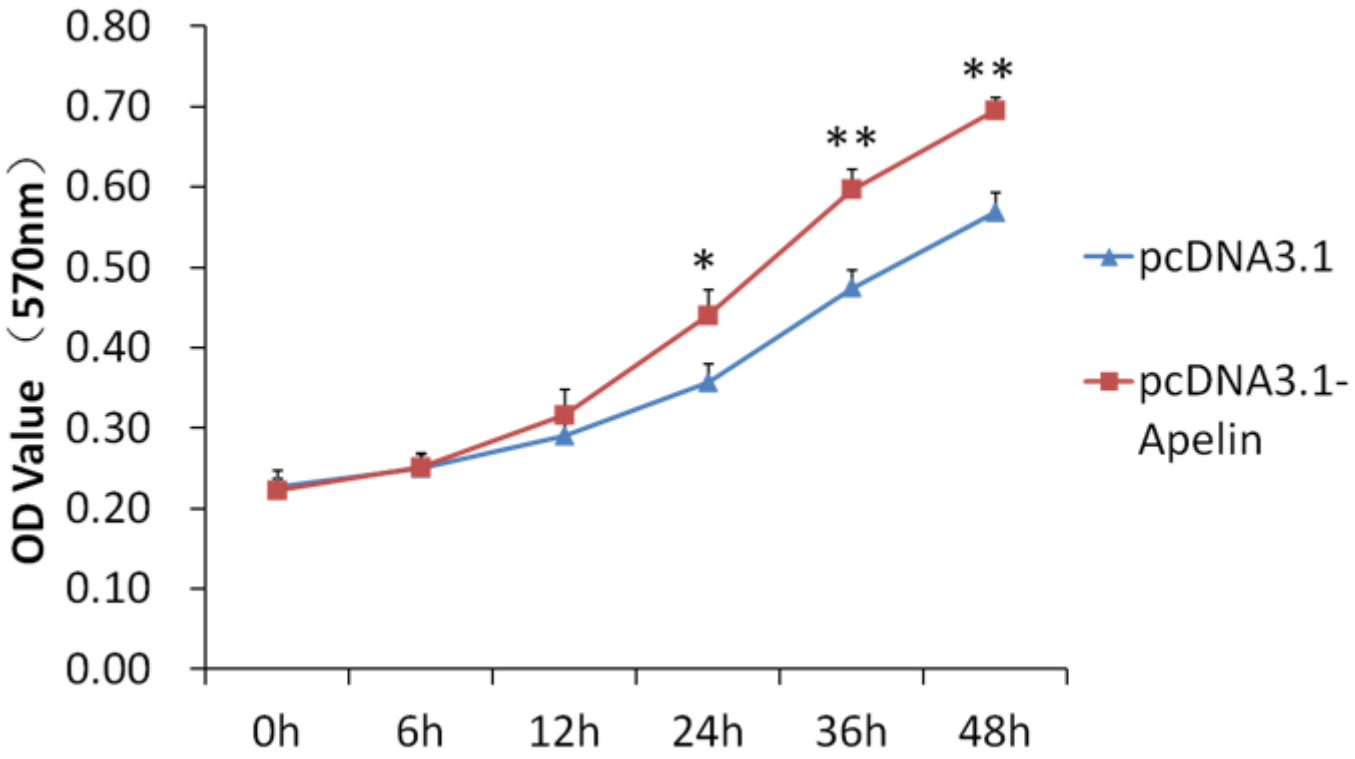

Figure 14

The proliferation after transfection by MTT assay. The proliferation of MGC-803 cells was measured transfected with pcDNA3.1-Apelin or pcDNA3.1 at different time point. (*Compared with the control group P□0.05, **Compared with the control group P□0.01).

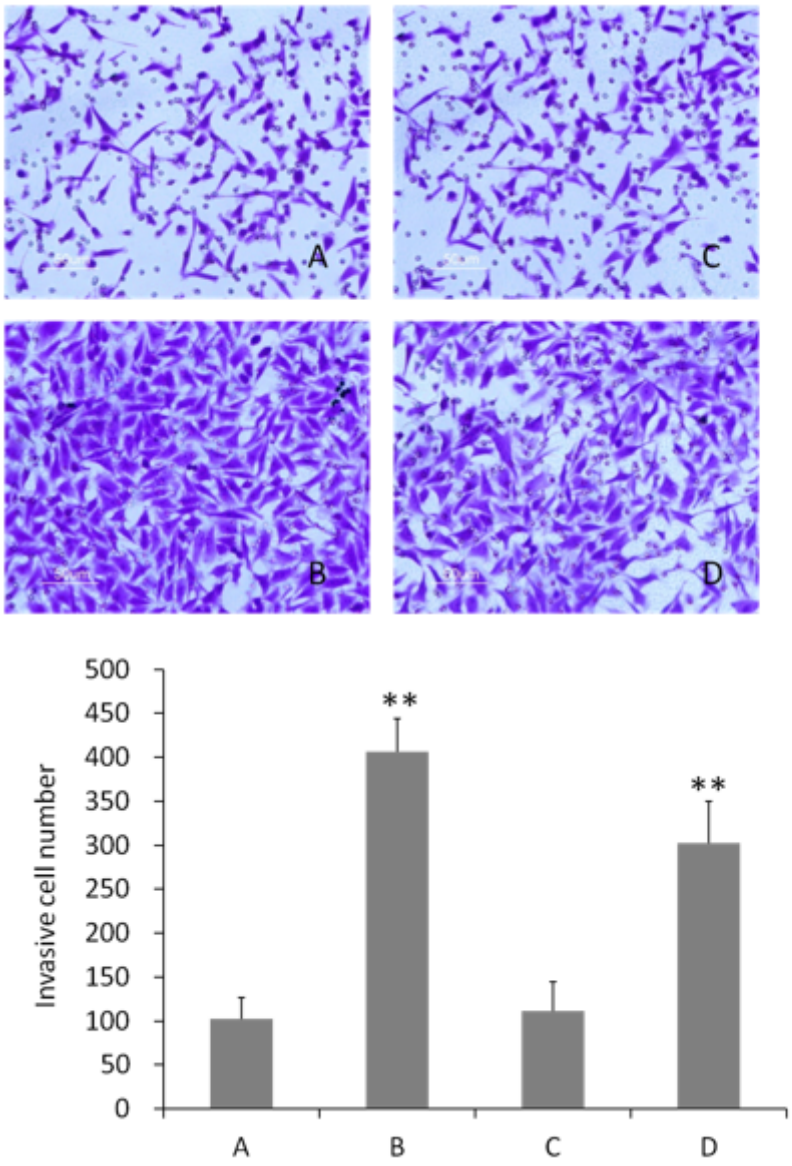

Figure 15

Effect of Apelin-13 induction and overexpression of Apelin on migration and invasion ability. Aimed at MGC-803 cells by Transwell assay. A：Untreated group; B:Apelin-13 induction group; C:pcDNA3.1 transfected cells; D：pcDNA3.1-Apelin transfected cells. (** Compared with the control group P＜0.01).

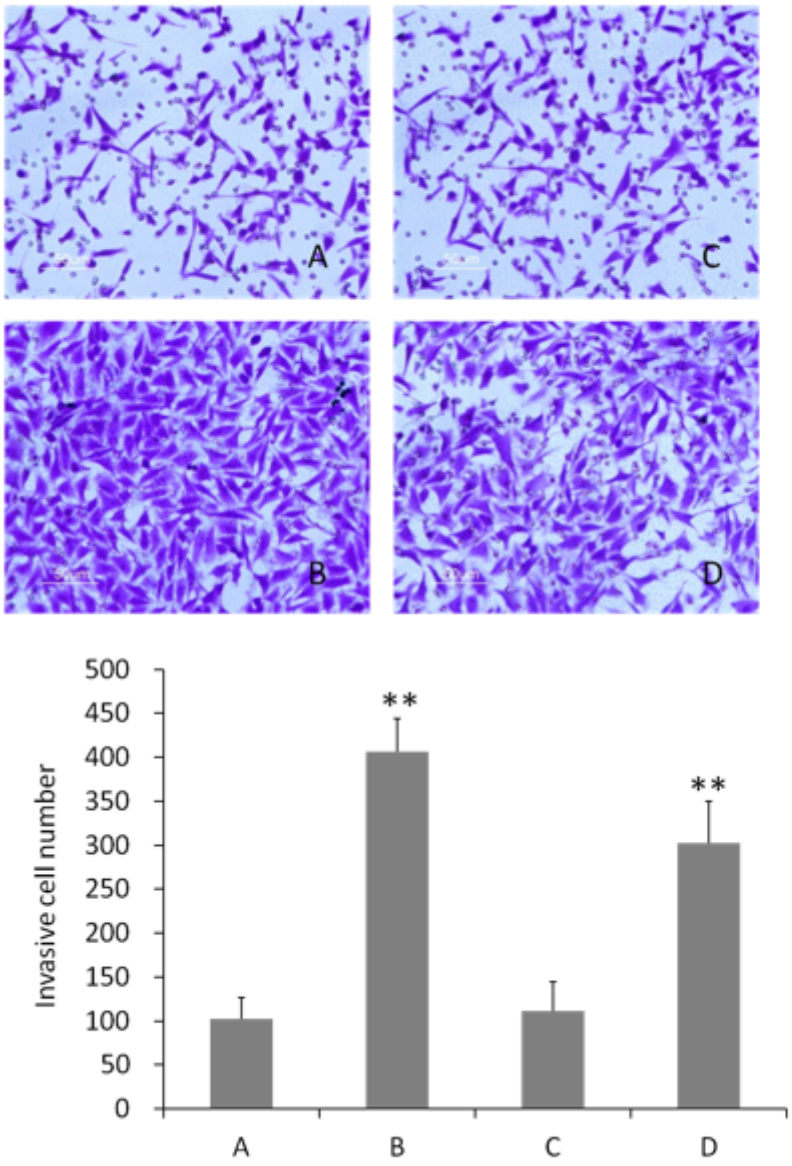

Figure 15

Effect of Apelin-13 induction and overexpression of Apelin on migration and invasion ability. Aimed at MGC-803 cells by Transwell assay. A：Untreated group; B:Apelin-13 induction group; C:pcDNA3.1 transfected cells; D：pcDNA3.1-Apelin transfected cells. (** Compared with the control group P＜0.01).

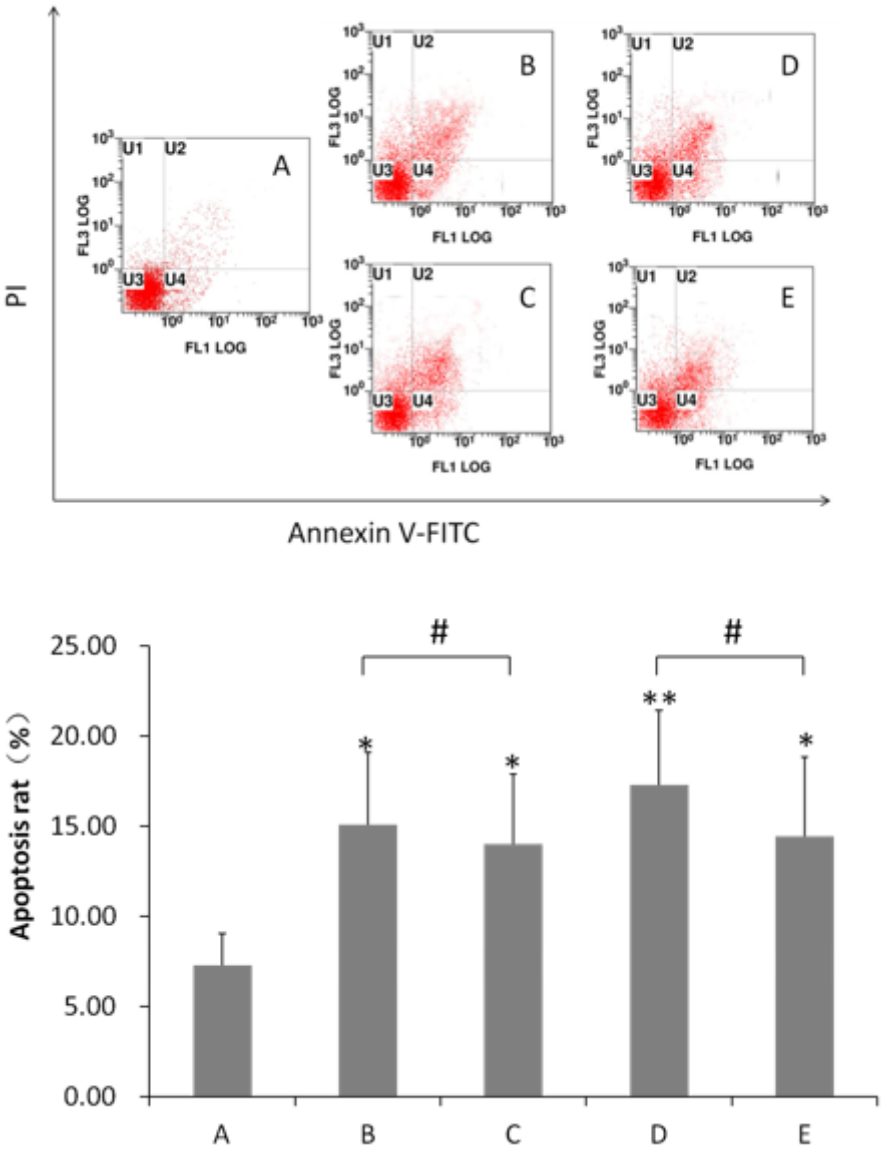

Figure 16

Effect of Apelin-13 induction and overexpression on apoptosis rate of MGC-803 cells by transwell assay. A：Untreated group; B：SAHA induction group; C：SAHA +Apelin-13 induction group; D：SAHA induction +pcDNA3.1 transfection group; E：SAHA induction+ pcDNA3.1-Apelin transfection group. * Compared with A group P＜0.05；** Compared with A group P＜0.01；# P＜0.05；

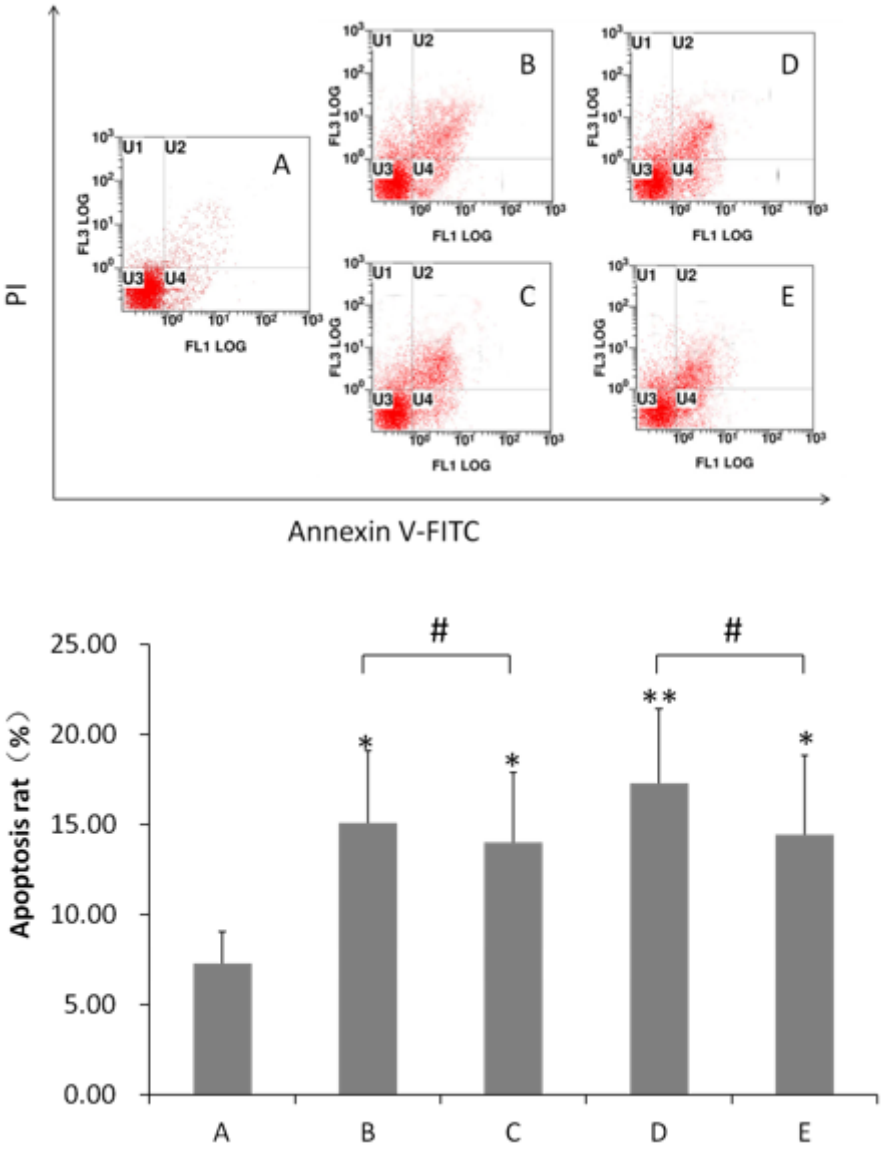

Figure 16

Effect of Apelin-13 induction and overexpression on apoptosis rate of MGC-803 cells by transwell assay. A：Untreated group; B：SAHA induction group; C：SAHA +Apelin-13 induction group; D：SAHA induction +pcDNA3.1 transfection group; E：SAHA induction+ pcDNA3.1-Apelin transfection group. * Compared with A group P＜0.05；** Compared with A group P＜0.01；# P＜0.05；

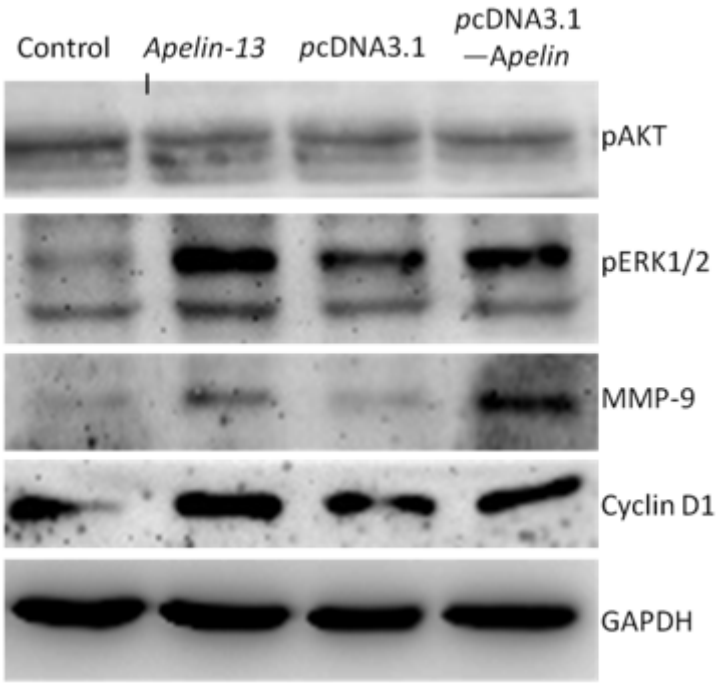

Figure 17

Western blot analysis of MGC-803 cells in different models. Including untreated cells, apeln-13 inducing cells (incubated with a concentration of 2.5μmol/L for 24 hours), mock-vector transfected cells (24 hours after transfection with pcDNA3.1 vector) and pcDNA3.1-Apelin transfected cells (24 hours after transfection with pcDNA3.1-Apelin vector)

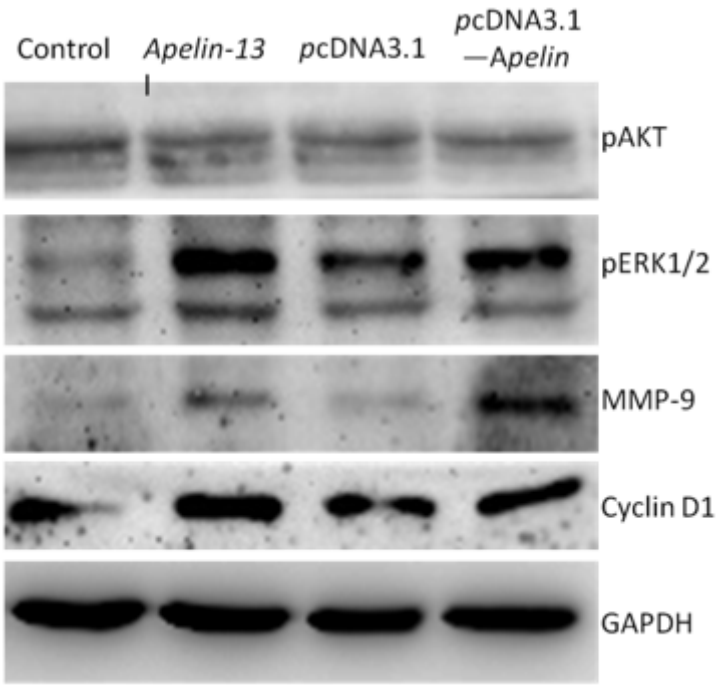

Figure 17

Western blot analysis of MGC-803 cells in different models. Including untreated cells, apeln-13 inducing cells (incubated with a concentration of 2.5μmol/L for 24 hours), mock-vector transfected cells (24 hours

after transfection with pcDNA3.1 vector) and pcDNA3.1-Apelin transfected cells (24 hours after transfection with pcDNA3.1-Apelin vector)

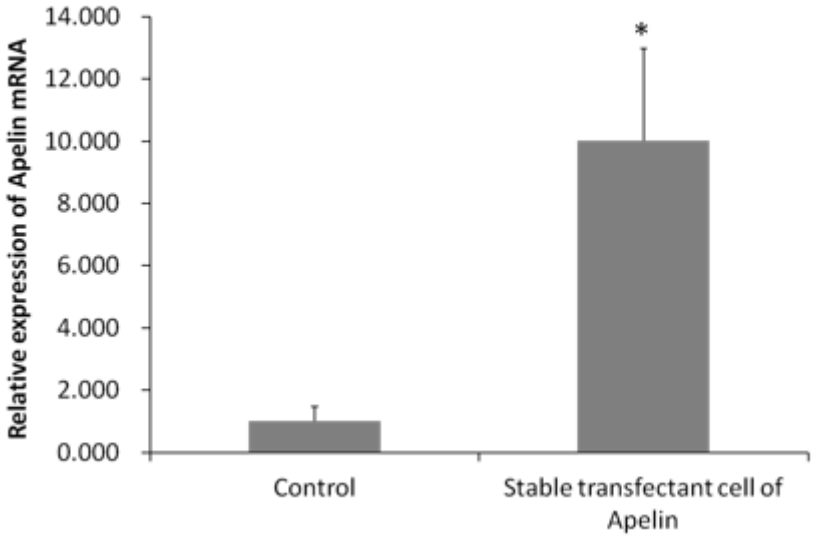

Figure 18

The relative expression levels of Apelin mRNA by RT-PCR analysis in vivo. There was a significant difference between stable transfected MGC-803 cells of over-expressed Apelin group and control□*P□ 0.05□

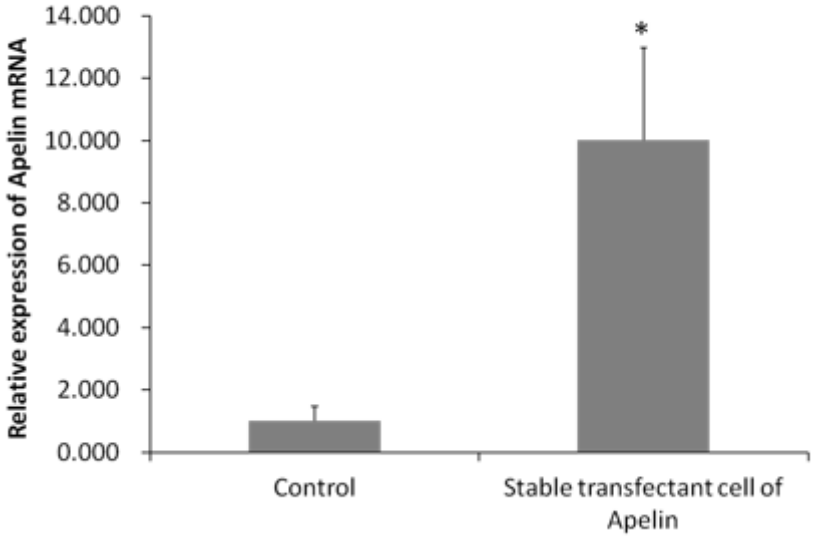

Figure 18

The relative expression levels of Apelin mRNA by RT-PCR analysis in vivo. There was a significant difference between stable transfected MGC-803 cells of over-expressed Apelin group and control□*P□ 0.05□

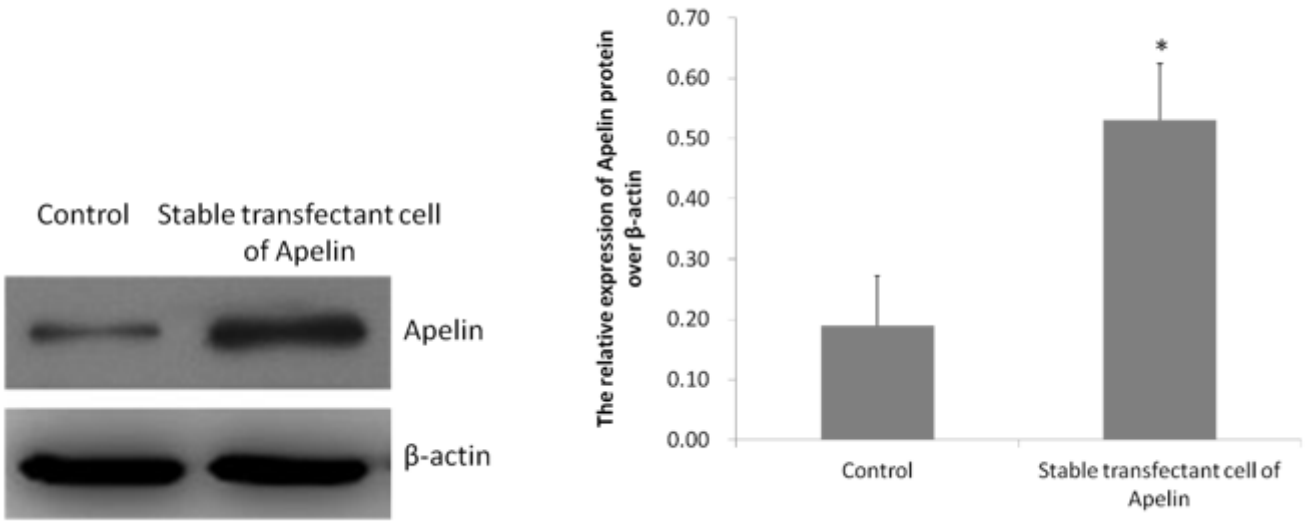

Figure 19

The relative expression levels of Apelin-encoding protein by Western blot analysis in vivo. There was a significant difference between stable transfected MGC-803 cells of over-expressed Apelin group and control（*P＜0.05）

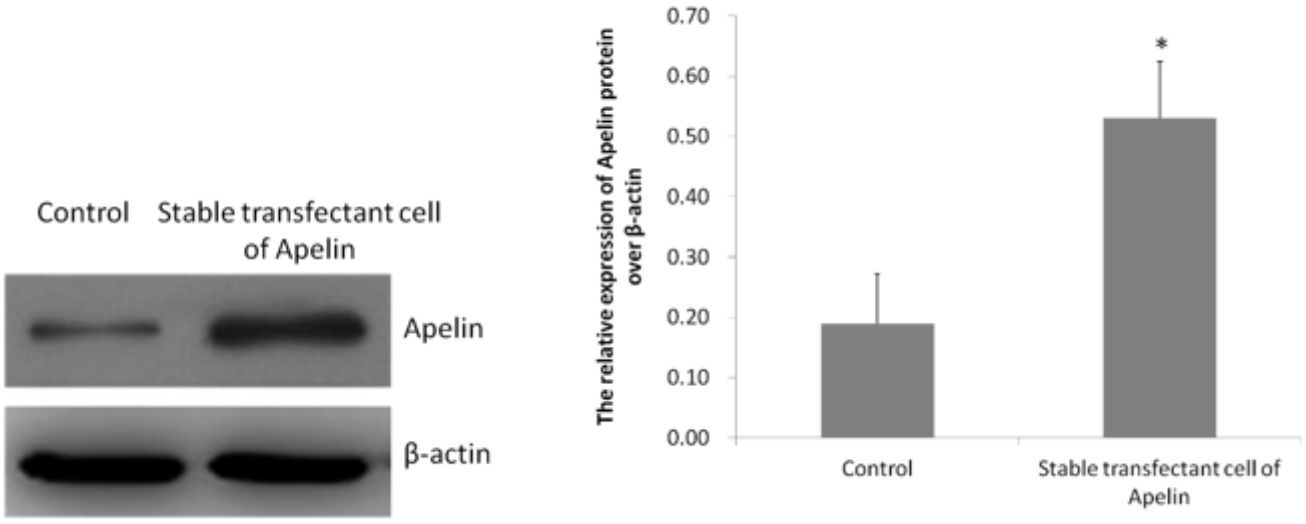

Figure 19

The relative expression levels of Apelin-encoding protein by Western blot analysis in vivo. There was a significant difference between stable transfected MGC-803 cells of over-expressed Apelin group and control（*P＜0.05）

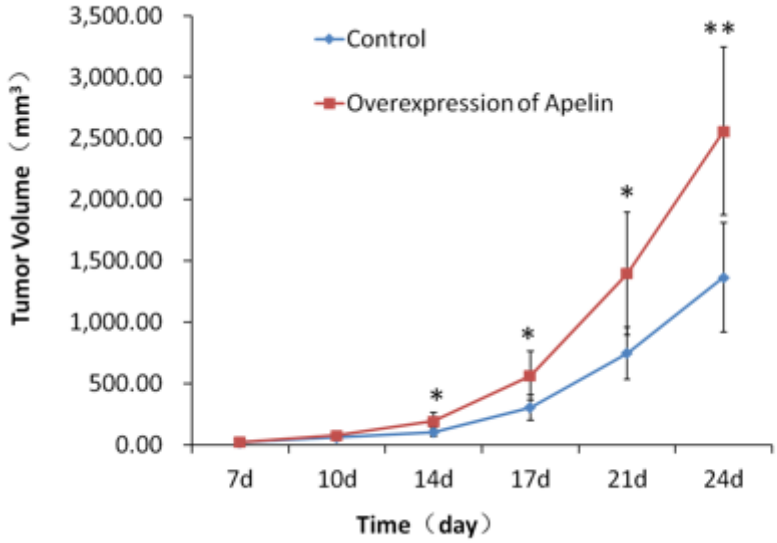

Figure 20

The tumor growth curves within 24 days in vivo. The subcutaneous over-expressed Apelin and control were separately injected into the nude mice. (*P□0.05□** P□0.01□

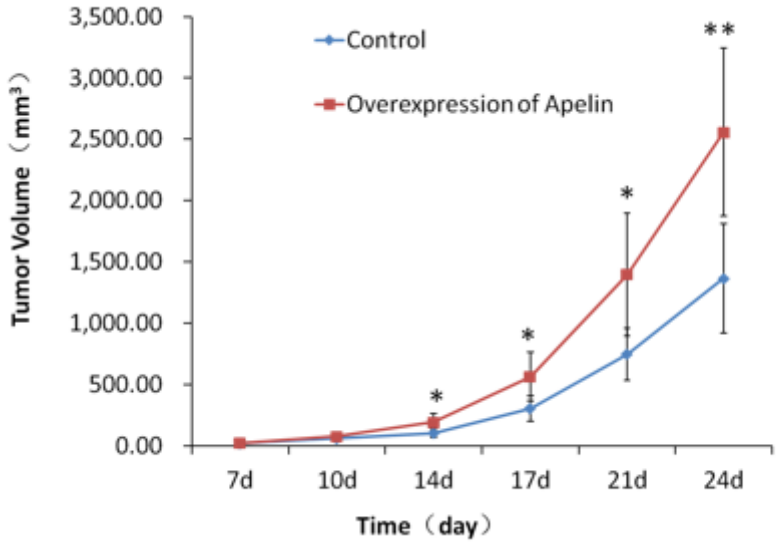

Figure 20

The tumor growth curves within 24 days in vivo. The subcutaneous over-expressed Apelin and control were separately injected into the nude mice. (*P□0.05□** P□0.01□

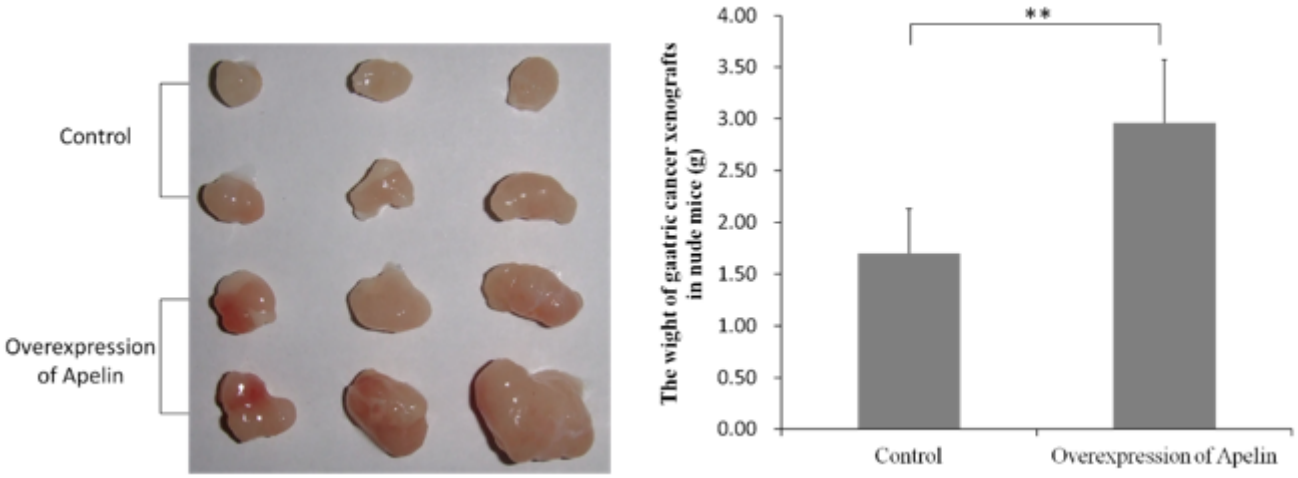

Figure 21

The gastric cancer xenografts in nude mice. (A) The xenografts removed from the mice. (B) Mean tumor weight of over-expressed Apelin and control tumors (** P□0.01)

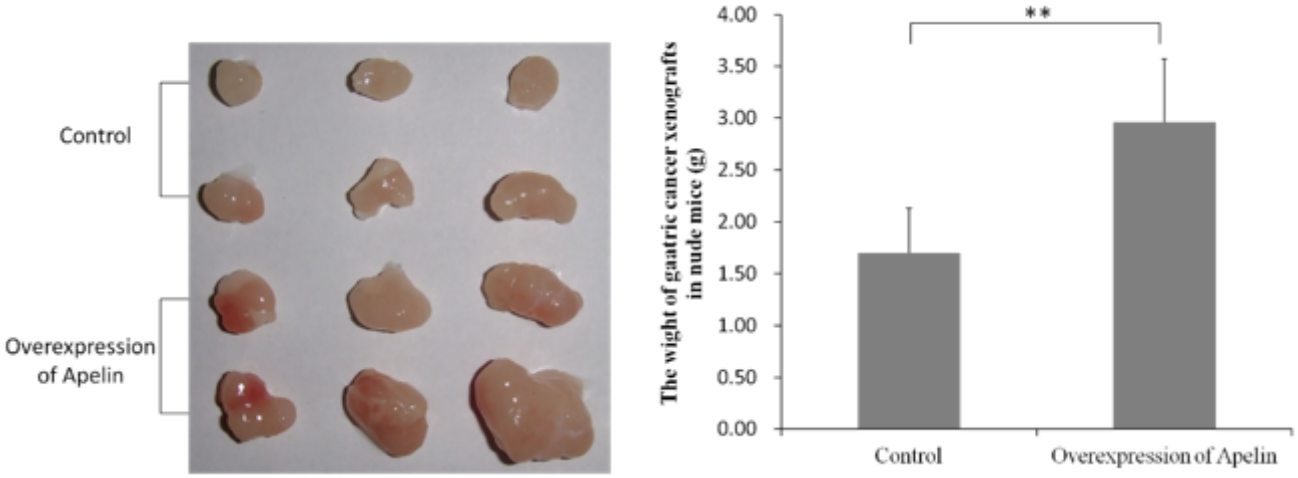

Figure 21

The gastric cancer xenografts in nude mice. (A) The xenografts removed from the mice. (B) Mean tumor weight of over-expressed Apelin and control tumors (** P□0.01)

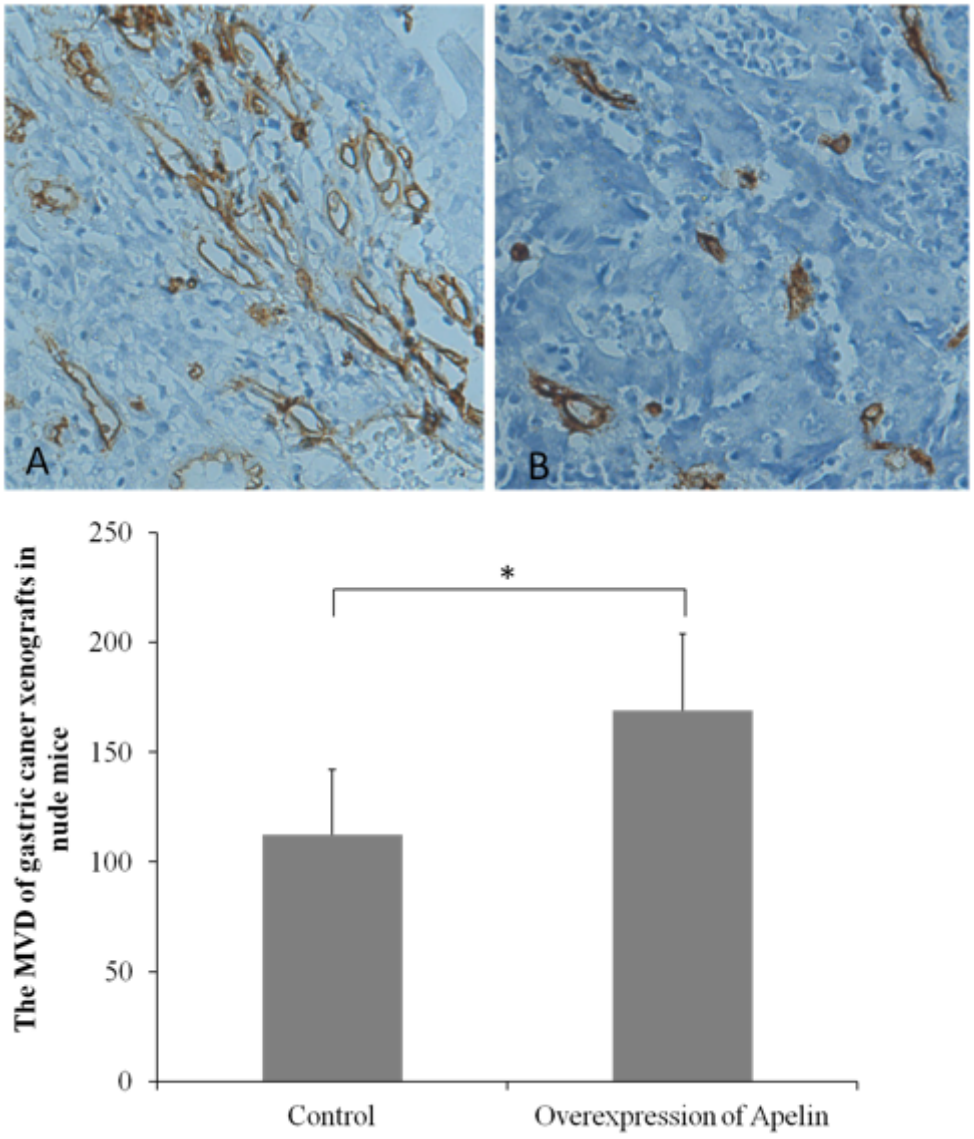

Figure 22

Detection of MVD in gastric cancer xenografts in nude mice（CD34 marked）magnification ×200（. A: Xenografts tumors with over-expressed Apelin; B: Xenografts tumor with control (*P（0.05).

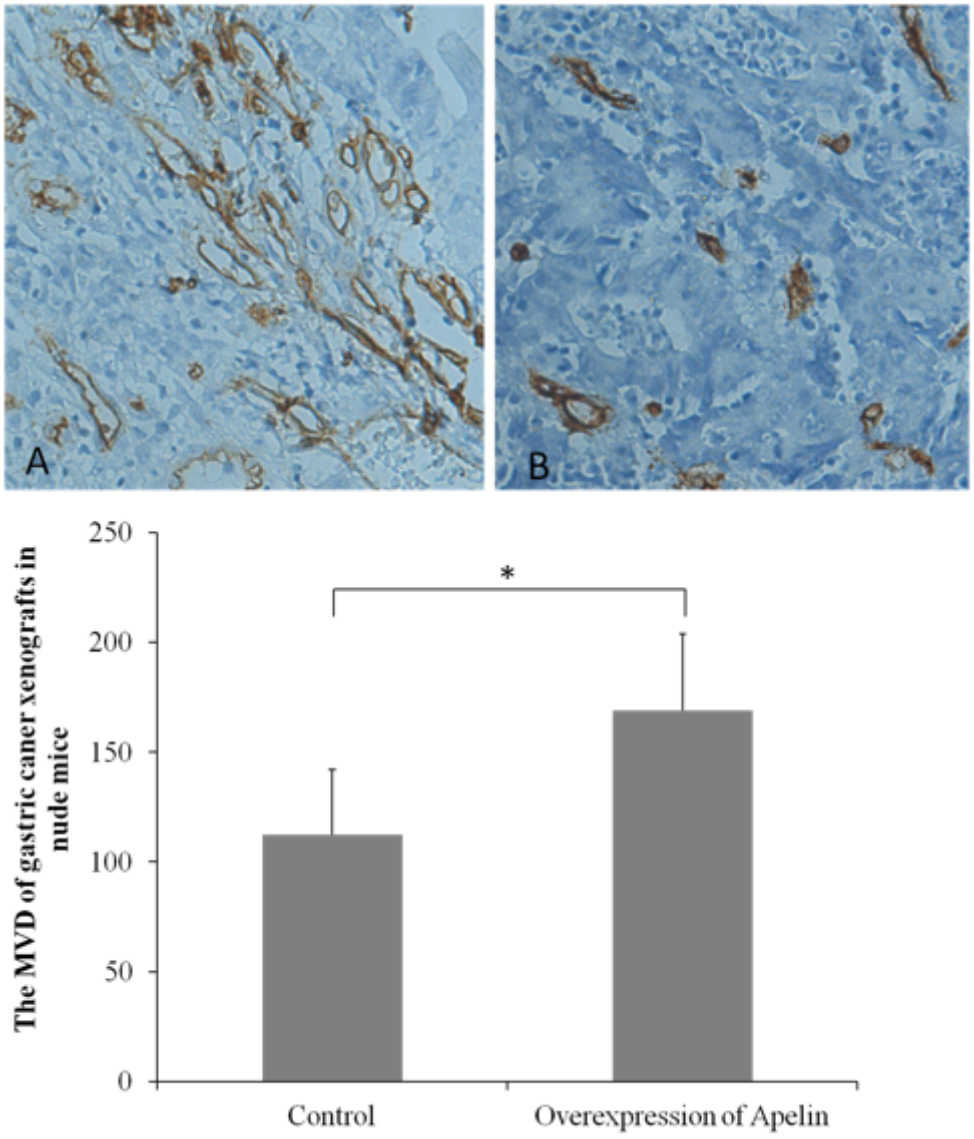

Figure 22

Detection of MVD in gastric cancer xenografts in nude mice（CD34 marked）magnification ×200）. A: Xenografts tumors with over-expressed Apelin; B: Xenografts tumor with control (*P＜0.05).